Biochimica et Biophysica Acta 1810 (2011) 1220–1229

Contents lists available at SciVerse ScienceDirect

Biochimica et Biophysica Acta

journal homepage: www.elsevier.com/locate/bbagen

Up-regulation of adenylylcyclases I and II induced by long-term adaptation of rats to morphine fades away 20 days after morphine withdrawal

Hana Ujcikova [a,b], Katerina Dlouha [a], Lenka Roubalova [a], Miroslava Vosahlikova [a], Dmytro Kagan [a], Petr Svoboda [a,b,*]

[a] Institute of Physiology, v.v.i., Academy of Sciences of the Czech Republic, Videnska 1083, 14220 Prague 4, Czech Republic
[b] Department of Physiology, Faculty of Science, Charles University, Vinicna 7, 12844 Prague 2, Czech Republic

ARTICLE INFO

Article history:
Received 21 April 2011
Received in revised form 12 September 2011
Accepted 27 September 2011
Available online 4 October 2011

Keywords:
Morphine
Long-term adaptation
Adenylyl cyclase isoforms I–IX
Forebrain cortex
Isolated plasma membranes

ABSTRACT

Background: Activation of adenylyl cyclase (AC) by prolonged exposure of mammalian organism to morphine was demonstrated in previous studies of mechanism of action of this drug. However, expression level of individual AC isoforms was not analyzed in crucial cell structure, plasma membrane (PM).
Methods: Rats were adapted to morphine for 10 days and sacrificed 24 h (group + M10) or 20 days (+M10/−M20) after the last dose. Control animals were sacrificed in parallel with morphine-treated (groups − M10 and (−M10/−M20)). Percoll®-purified PM were isolated from brain cortex and analyzed by immunoblotting and specific radioligand binding.
Results: ACI (ACII) was increased 8× (2.5×) in morphine-adapted rats (+M10) when compared with controls (−M10). Increase of ACI and II by long-term adaptation to increasing doses of morphine represented a specific effect as the amount of ACIII–ACIX, of prototypical PM marker, Na, K-ATPase and of trimeric G protein α and β subunits was unchanged. Increase of ACI and II was not detected in PM isolated from group (+M10/−M20). Thus, the marked increase of ACI and ACII faded away 20 days since the last dose of morphine.
Conclusions: We assume that the specific increase in expression level of ACI and ACII in brain cortex of morphine-adapted rats proceeds as a compensatory, homeostatic response to prolonged exposure to inhibitory drug, morphine.
General significance: Our findings demonstrate that the *dramatic and specific* change of the crucial component of the opioid receptor cascade in brain cortex, manifested as an increase in PM level of ACI and II, is reversible.

1. Introduction

Physiological action of opioid drugs requires an initial interaction with opioid receptors [1]. These receptors, MOR (μ-OR), DOR (δ-OR) and KOR (κ-OR) [2–9] are classified as members of rhodopsin family of G-protein coupled receptors, GPCRs. All these receptors are known to inhibit adenylyl cyclase activity in pertussis-toxin-dependent manner by activation of G_i/G_o class of trimeric G proteins [10]. These proteins (G_i1, G_i2, G_i3, G_o1, G_o2) are present in brain in large quantities and inhibit adenylyl cyclase activity or regulate ionic channels in pertussis-toxin-dependent manner [11–15].

Hyper-sensitization or super-activation of AC enzyme activity by prolonged exposure of cultured cells or mammalian organisms to morphine has been demonstrated in previous studies of mechanism of action of this drug representing the non-selective OR agonist [1,7,8,16–26]. Adenylyl cyclase is regulated by trimeric G-proteins, so any significant change of AC activity should be preceded by alternation of trimeric G-protein activity.

In our previous work [27], the purified membranes from brain cortex were used for determination of DAMGO (μ-OR)-, DADLE (δ-OR)-, and U-23554 (κ-OR)-stimulated [^{35}S] GTPγS binding which was used as an estimate of trimeric G protein activity. Membranes were isolated from forebrain cortex of control and morphine-treated rats. Results of this study indicated a clear desensitization of DAMGO- and DADLE-stimulated G protein response in membranes prepared from

Abbreviations: AC, adenylyl cyclase; β-AR, β-adrenergic receptor; DADLE, [2-D-alanine, 5-D-leucine]enkephalin = Tyr-D-Ala-Gly-Phe-D-Leu; DAMGO, [2-D-alanine, 4-N-methylphenylalanine, 5-glycinol]enkephalin = Tyr-D-Ala-Gly-N-methyl-Phe-Gly-ol; DOR, δ-opioid receptor; GPCR, G protein-coupled receptor; G proteins, heterotrimeric guanine nucleotide-binding regulatory proteins; $G_s\alpha$, G protein α subunit stimulating adenylyl cyclase activity; $G_i/G_o\alpha$, G protein α subunits inhibiting adenylyl cyclase activity in pertussis-toxin sensitive manner; $G_q/G_{11}\alpha$, G protein α subunits stimulating phoshoplipase C in pertussis-toxin independent manner; [^{35}S]GTPγS, guanosine-5′-[γ-^{35}S] triphosphate; KOR, κ-opioid receptor; PM, plasma (cell) membranes; MOR, μ-opioid receptor; Na,K-ATPase, sodium- plus potassium-activated, ouabain-dependent adenosine triphosphatase (EC 3.6.1.3); P_i, inorganic phosphate; OR, opioid receptor; PBS, phosphate-buffered saline; PM, plasma membrane; PMSF, phenylmethylsulfonyl fluoride; PTX, pertussis toxin; SLB, sample loading buffer; TBS, Tris-buffered saline; w.w., wet weight

* Corresponding author at: Institute of Physiology, Academy of Sciences of the Czech Republic, Videnska 1083, 14220 Prague 4, Czech Republic. Tel.: +420 2 41062533; fax: +420 2 41062488.
E-mail address: svobodap@biomed.cas.cz (P. Svoboda).

0304-4165/$ – see front matter © 2011 Elsevier B.V. All rights reserved.
doi:10.1016/j.bbagen.2011.09.017

morphine-treated rats [27]. U-23554-stimulated [^{35}S] GTPγS binding was unchanged. Our results were fully in line with data of Sim et al. [28], Sim-Selley et al. [29] and Maher et al. [30] indicating the desensitization of G protein response in specific areas of brain stem and hippocampus in morphine- as well as heroine-adapted rats.

In our present work, we have analyzed the content of *all* types of adenylyl cyclase protein molecules (ACI–IX) in PM isolated in the same way from morphine-adapted rats because the previous analyses of AC in drug-addicted state were preferentially oriented to functional assays of AC only and not to the quantitative determination of different isoforms of this enzyme in plasma membranes. Recent histochemical analysis of ACI–IX mRNA levels indicated that the expression level of ACI and II in rat brain cortex is high [31].

2. Material and methods

2.1. Chemicals

[^{3}H]-ouabain (30 mCi/mmol, NET211001MC), [^{3}H]DADLE (39.1 Ci/mmol, NET648250UC) and [^{3}H]DPDPE (45 Ci/mmol; NET922050UC) were purchased from Perkin Elmer. [α-^{32}P] ATP (adenosine-5′-[α-^{32}P] triphosphate, cat. no. 32007.2) was purchased from MP Biomedicals. [^{3}H]cAMP (cyclic 3′,5′-[α-^{3}H] adenosine monophosphate, cat. no. TRK498) was from Amersham. Complete protease inhibitor cocktail was from Roche Diagnostic, Mannheim, Germany (cat. no. 1697498). All other chemicals were of highest purity available.

2.2. Antisera

$G_i\alpha$ and $G_o\alpha$ subunit proteins were identified by antipeptide antibodies as originally described by Gierschik et al. [11], Goldsmith et al. [12], Backlund et al. [13] and Milligan [15]. Production of the rabbit polyclonal antisera anti-$G_i1/G_i2\alpha$, anti-$G_i3\alpha$, anti-G_o and anti-$G_q/G_{11}\alpha$ was performed according to Mitchell et al. [32,33], Mullaney and Milligan [34] and Mullaney et al. [35–37]. These antisera were previously characterized in our laboratory by Ihnatovych [38]. $G_s\alpha$ (G-5040) antibody was from Sigma. Rabbit polyclonal antibodies $G_z\alpha$ (I-20, sc-388), Gβ (T-20, sc-378), ACI (V-20, sc-586), ACII (C-20, sc-587), ACIII (C-20, sc-588), ACIV (C-20, sc-589), ACV/VI (C-17, sc-590), ACVII (M-20, sc-1966), ACVIII (C-17, sc-32131), ACIX (N-18, sc-8576) were purchased from Santa Cruz Biotechnology. Antibody oriented against α subunit of Na, K-ATPase (H-300, sc-28800) was also from Santa Cruz. Caveolin-1-oriented antibody C13630 was purchased from Transduction Laboratories [39].

2.3. Animals

All experiments were performed in accordance with the European Council Directive (86/609/EEC). Male Wistar rats (220–250 g) were killed by decapitation under ether narcosis, the frontal brain was rapidly removed, washed intensively from the remaining blood and cooled to 0 °C. The cerebral cortex was separated on the pre-cooled plate, snap frozen in liquid nitrogen and stored at −70 °C until use.

2.4. Morphine treatment of experimental animals

The animals were exposed to morphine by intra-muscular application according to the following protocol: 10 mg/kg (days 1 and 2), 15 mg/kg (days 3 and 4), 20 mg/kg (days 5 and 6), 30 mg/kg (days 7 and 8), 40 mg/kg (day 9) and, finally 50 mg/kg (day 10). The morphine-adapted rats were sacrificed 24 h (group + M10) or 20 days (group (+M10/−M20)) after the last dose of the drug. Control animals were injected with sterile PBS and sacrificed in parallel with morphine-adapted rats, i.e. 24 h (−M10) or 20 days (−M10/−M20) after the last dose.

An independent group of animals was exposed to the single dose (injection) of 10 mg/kg, 15 mg/kg, 20 mg/kg, 30 mg/kg, 40 mg/kg or 50 mg/kg of morphine (group + M1) and sacrificed for 24 h later. Control animals were injected with sterile PBS (group − M1). The aim of this *short term morphine exposure* experiment was to obtain an independent set of data on ACI and II levels in PM with the aim to compare these data with those collected from *morphine-adapted* rats for 10 days (group + M10).

2.5. Isolation of plasma membrane-enriched fraction from rat brain cortex

Rat brain cortex was minced with razor blade on pre-cooled plate and diluted in STEM medium containing 250 mM sucrose, 20 mM Tris–HCl, 3 mM $MgCl_2$, 1 mM EDTA, pH 7.6, fresh 1 mM PMSF plus protease inhibitor cocktail. It was then homogenized mildly in loosely-fitting Teflon-glass homogenizer for 5 min (2 g w. w. per 10 ml) and centrifuged for 5 min at 3500 rpm. Resulting post-nuclear supernatant (PNS) was filtered through Nylon nets of decreasing size (330, 110 and 75 mesh, Nitex) and applied on top of Percoll in Beckman Ti70 tubes (30 ml of 27.4% Percoll in STE medium). Centrifugation for 60 min at 30,000 rpm (65,000×*g*) resulted in the separation of two clearly visible layers [40]. The upper layer represented plasma membrane fraction (PM); the lower layer contained mitochondria (MITO). The upper layer was removed, diluted 1:3 in STEM medium and centrifuged in Beckman Ti70 rotor for 90 min at 50,000 rpm (175,000×*g*). Membrane sediment was removed from the compact, gel-like sediment of Percoll and re-homogenized by hand in a small volume of 50 mM Tris–HCl, 3 mM $MgCl_2$, 1 mM EDTA, pH 7.4 (TME medium).

2.6. SDS-PAGE and immunoblotting

The aliquots of membrane fractions were mixed 1:1 with 2× concentrated Laemmli buffer (SLB) and heated for 3 min at 95 °C. Standard (10% w/v acrylamide/0.26% w/v bis-acrylamide) SDS electrophoresis was carried out as described before [41–43]. Molecular mass determinations were based on pre-stained molecular mass markers (Sigma, SDS 7B). After SDS-PAGE, proteins were transferred to nitrocellulose and blocked for 1 h at room temperature in 5% (w/v) low-fat milk in TBS-Tween buffer [10 mM Tris–HCl, pH 8.0, 150 mM NaCl, 0.1% (v/v) Tween 20]. Antibodies were added in TBS-Tween containing 1% (w/v) low-fat milk and incubated for at least 2 h. The primary antibody was then removed and the blot washed extensively (3×10 min) in TBS-Tween. Secondary antibodies (donkey anti-rabbit IgG conjugated with horse-radish peroxidase) were diluted in TBS-Tween containing 1% (w/v) low-fat milk, applied for 1 h and after three 10 min washes the blots were developed by ECL technique using Super Signal West Dura (Pierce) as substrate. The developed blots were scanned with an imaging densitometer ScanJett 5370C (HP) and quantified by Aida Image Analyzer v. 3.28 (Ray test).

When indicated, membrane fractions were also analyzed by NuPAGE system (Invitrogen). Aliquots of membrane fractions were solubilized in NuPAGE LDS Sample Buffer (4×) with addition of NuPAGE Sample Reducing Agent (10×) according to manufacturer's instructions. Samples were heated at 70 °C for 10 min, loaded at 10 μg/well and resolved by NuPAGE 4–12% or 10% Bis-Tris polyacrylamide gels (10 wells,1 mm thick) using 3-(N-morpholino) propane sulfonic acid (MOPS), sodium dodecyl sulfate (SDS) running buffer with NuPAGE Antioxidant prior to blotting on nitrocellulose membranes (Protran, Schleicher & Schuell). Western blotting was carried out as described above.

2.7. Na, K-ATPase

All membrane preparations were screened for the content of PM marker, sodium- plus potassium-activated magnesium-dependent adenosine triphosphatase (EC 3.6.1.3). Na, K-ATPase was determined

by binding of radioactively labeled, selective inhibitor of this enzyme, [^{3}H]ouabain as described before by Svoboda et al. [44]. Membranes (50 μg) were incubated with 5 nM [^{3}H]ouabain for 90 min at 30 °C in total volume of 0.4 ml of 5 mM $NaHPO_4$, 5 mM $MgCl_2$, 50 mM Tris–HCl, pH 7.6 at 37 °C. Binding reaction was terminated by dilution with 5 ml of ice-cold buffer and filtration through Whatman GF/B filters. The filters were washed twice, dried overnight at laboratory temperature and the radioactivity was determined by liquid scintillation. Non-specific binding was determined in the presence of 1 μM unlabelled ouabain.

Membrane density of Na, K-ATPase molecules was detected by immunoblotting with antibodies oriented against α-subunit of this enzyme (sc-28800, Santa Cruz) as described above.

2.8. Adenylyl cyclase

Adenylyl cyclase enzyme activity was determined as described before by Bourova et al. [45]. Reaction mix was prepared according to Salomon [46]; separation of cyclic AMP from other nucleotides and inorganic phosphate was performed by dry alumina column chromatography as described by White [47].

2.9. δ-opioid receptors

Saturation binding experiments were performed using [^{3}H]DADLE or [^{3}H]DPDPE according to Bourova et al. [45] and Moon et al. [48]. The assay medium contained membrane protein (120 μg per tube) diluted in final volume of 100 μl of binding mix containing 50 mM Tris–HCl, 10 mM $MgCl_2$, 1 mM EDTA, pH 7.4 ± 100 mM NaCl plus increasing radioligand concentrations ([^{3}H]DADLE 0.1–34.4 nM; [^{3}H]DPDPE 0.1–57.3 nM). Specific binding of the radioligand was obtained as the difference between binding in the absence and presence of nonradioactive 10 μM DADLE or DPDPE. After incubation for 60 min at 30 °C, samples were diluted with 3 ml of ice-cold Mg-HEPES buffer, immediately filtered and washed 3× with 3 ml of Mg-HEPES buffer. Whatman GF/B filters mounted in Brandel cell harvester were used for separation of bound and free radioactivity. Radioactivity remaining on the filters was determined by liquid scintillation. Data were analyzed by GraphPad*Prizm4*.

2.10. Protein determination

The method of Lowry was used for determination of membrane protein. Bovine serum albumin (Sigma, Fraction V) was used as standard. Data were calculated by fitting the data with calibration curve as quadratic equation.

3. Results

3.1. Morphine-induced increase in plasma membrane density of adenylylcyclases I and II

The amount of adenylylcyclases I and II was determined first in plasma membrane fraction (PM) isolated from frontal brain cortex of rats adapted to increasing doses of morphine for 10 days and compared with PM isolated from control animals. Data presented in Fig. 1A (left panels) indicate clearly a large increase in membrane density of ACI. Quantitative analysis of 32 immunoblots performed with 50 μg or 100 μg of PM protein applied per gel indicated a highly significant difference between the two sets of data, $p<0.001$. Membranes isolated from morphine-adapted rats (group + M10) exhibited 8× higher density of ACI than membranes isolated from control animals (group − M10). The same type of analysis, when performed with ACII oriented antibody indicated 2.5× increase of this enzyme protein in membranes prepared from morphine-adapted rats when compared with controls (Fig. 1A, middle panels). The difference between the two groups was again highly significant, $p<0.01$.

The increased level of ACI and ACII in PM samples prepared from morphine-adapted animals was not observed in membranes isolated from animals exposed to morphine for 10 days but sacrificed 20 days since the last dose of morphine (group (+M10/−M20)), Fig. 1B. These samples exhibited the same amount of ACI and ACII as corresponding controls (group (−M10/−M20)); (compare left and middle panels in Fig. 1B). Thus, in drug addicted state, PM density of AC molecules was dramatically increased mainly as far as ACI isoform was involved. This increase, being clearly disproportionate between ACI (8×) and ACII (2.5×), faded away 20 days since application of the last dose of morphine. Obviously, the withdrawal of the drug for sufficiently long period of time resulted in reversal of the pathological change back to "normal" state as far as the levels of these two isoforms of AC were involved.

The increase of ACI and II observed after 10 days of adaptation to increasing doses of morphine represented the specific phenomenon as the PM level of ACIII, IV, V/VI, VII, VIII and IX was unchanged (Fig. 2A). Furthermore, analysis of ACI and II in membranes prepared from animals exposed to the same doses of morphine but for 24 h only, i.e. to the *single* injection of morphine 10, 15, 20, 30, 40 and 50 mg/kg (see Material and methods for details), indicated that this short-term exposure had no effect on the membrane density of ACI and ACII in brain cortex PM (Fig. 2B). Thus, the dramatic and specific increase of ACI (8×) observed after 10 days of step-wise adaptation to increasing doses of morphine does not represent an acute phenomenon and may be regarded as the long-term adaptation of experimental animals to this drug.

3.2. Unchanged level of Na, K-ATPase

The next part of our work was oriented to analysis of other PM signaling molecules distinct from AC. Therefore, in parallel membrane samples to those used for determination of ACI and ACII, the specific content of Na, K-ATPase was measured as a negative standard and prototypical plasma membrane marker which should not be affected by morphine treatment, (Fig. 1A–C, right panels). Quantitative analysis of immunoblot signals corresponding to α subunit of this enzyme indicated that the expression level of this protein in PM was unchanged after adaptation to morphine for 10 days (Fig. 1A). Accordingly, the membrane content of Na, K-ATPase in samples isolated from rats sacrificed 20 days after the last dose of morphine was the same as in controls (Fig. 1B, right panel).

Data obtained by immunoblot analysis of Na, K-ATPase protein content in PM were extended and verified by analysis of "functional" parameter of this marker molecule, the number and affinity of binding sites for its selective inhibitor [^{3}H] ouabain. The maximum number (B_{max}) and affinity (K_d) of binding of this radioligand represents the highly selective and sensitive method for detection of Na, K-ATPase molecules in a given membrane sample. Virtually the same results as those obtained by immunoblot analysis were obtained (Fig. 3). Maximum binding capacity B_{max} and dissociation constant K_d of this radioligand binding to membranes isolated from morphine-adapted rats ($B_{max} = 35.5 \pm 2.1$ pmol . mg^{-1}; $K_d = 20.8 \pm 2.3$ nM) were not different from those determined in membranes prepared from control animals ($B_{max} = 36.6 \pm 2.1$ pmol . mg^{-1}; $K_d = 26.2 \pm 3.1$ nM).

3.3. Unchanged level of trimeric G protein α and β subunits

Determination ACI–IX and Na, K-ATPase presented in the previous paragraphs (Figs. 1–3) was accompanied by analysis of G protein content in PM preparations isolated from the same rats as those used for determination of ACI and ACII. The reason why we have performed this analysis was that the change in functional activity of a given set of signaling molecules does not necessarily mean the change in its expression level or membrane density. As already mentioned in introduction section, our previous data indicated the desensitization of G

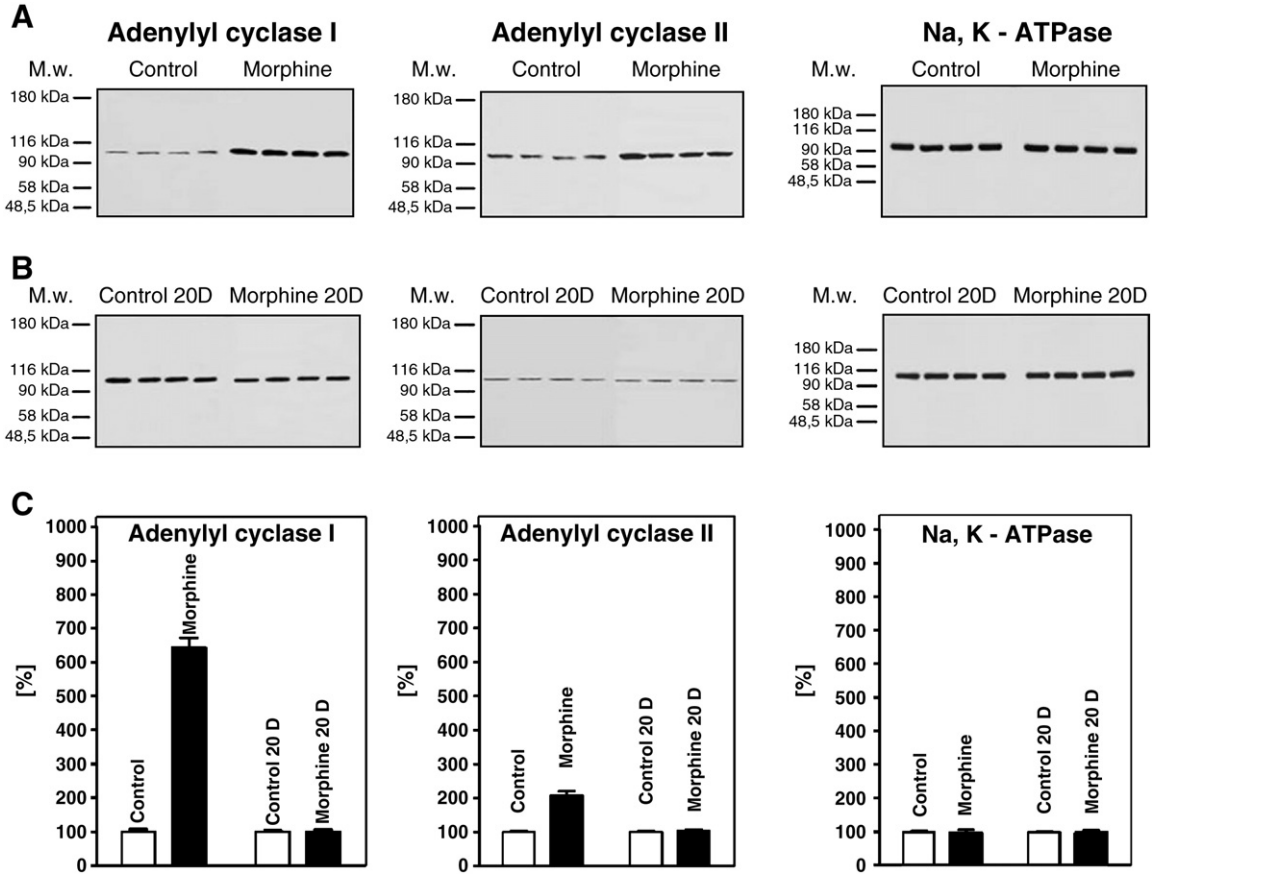

Fig. 1. Adenylyl cyclases I, II and Na, K-ATPase; *immunoblot analysis*. A. Membrane content of ACI (left), ACII (middle) and Na,K-ATPase (right panels) was determined by quantitative immunoblotting in PM isolated in parallel from brain cortex of control rats (group − M10) and rats adapted to increasing doses of morphine for 10 days (group + M10). Adaptation was performed according to the following protocol: 10 mg/kg (days 1 and 2), 15 mg/kg (days 3 and 4), 20 mg/kg (days 5 and 6), 30 mg/kg (days 7 and 8), 40 mg/kg (day 9) and 50 mg/kg (day 10). Control animals were injected with PBS at the same time intervals. Resolution of control and morphine-adapted samples by SDS-PAGE was always performed on the same gel and subsequently transferred to the same nitrocellulose sheet. Typical immunoblots performed with the same amount of protein in the two types of PM are shown: 4×(−M10) samples followed by 4×(+M10) samples from left to right. Control, membranes isolated from group (−M10); Morphine, membranes isolated from group (+M10). B. PM had been isolated from animals adapted to morphine according to the same protocol but further nurtured for 20 days in the absence of this drug (group (+M10/−M20)). Corresponding controls were represented by PM isolated from animals designated as (−M10/−M20), see Material and methods. Animals in this group were injected with PBS for 10 days and subsequently nurtured in the absence of any additions/injections for 20 days. Typical immunoblots performed with the same amount of PM protein resolved in the same gel [4×(−M10) plus 4×(+M10) samples] are shown. Control 20D, membranes isolated from group (−M10/−M20); Morphine 20D, membranes isolated from group (+M10/−M20). C. Statistical analysis of immunoblot signals collected from 32 (ACI), 26 (ACII) and 12 (Na, K-ATPase) immunoblots [4×(−M10) plus 4×(+M10) samples in each gel/blot]. Numbers represent the average + M10/−M10 ratio ± SEM expressed as% of control values, 100%.

protein response to OR stimulation in membranes isolated from morphine-adapted rats [27].

Data presented in Fig. 4 indicated clearly the unchanged level of all the major classes of trimeric G protein α and β subunits: $G_i1/G_i2\alpha$, $G_i3\alpha$, $G_o\alpha$, $G_z\alpha$, $G_s\alpha$, $G_q/G_{11}\alpha$ and Gβ. When normalized and compared in at least 3 immunoblots performed with different amounts of protein, the difference between morphine-treated and control samples (100%) was not significant: $G_i1/G_i2\alpha$ (100 ± 10%), $G_i3\alpha$ (109 ± 5%), $G_o\alpha$ (105 ± 2%), $G_z\alpha$ (100 ± 6%), $G_s\alpha$ (98 ± 4%), $G_q/G_{11}\alpha$ (96 ± 4%), Gβ (101 ± 7%). Membrane density of caveolin-1 was also unchanged — the level of this PM marker in morphine-adapted samples represented 89 ± 6% of the control level. The difference between control and morphine treated rats was analyzed by Student's *t*-test and expressed as% of control level. The numbers represent the average ± SEM of densitometric scans carried out in triplicate.

Results presented in Fig. 4 may be regarded as an additional support for desensitization mechanism of morphine action as more drastic adaptation should result in decrease of the amount of the cognate G protein α subunits in PM isolated from morphine-treated rats. This phenomenon, known as *down-regulation* of G proteins is well known, has been originally described by Milligan and Green [49] in white fat cells and later demonstrated in numerous GPCR-stimulated cascades both in cultured cells and intact tissue [35,36,49–56].

3.4. Adenylyl cyclase activity in morphine-adapted rats

The question, to what extend the increase of ACI and ACII in brain cortex of morphine-adapted rats (group + M10) is associated with or reflected in change of an overall adenylyl cyclase enzyme activity, was tested in parallel PM samples as those used before in immunoblot analysis of ACI–IX, Na, K-ATPase and G protein subunits. Data shown in Fig. 5 indicated that inhibitory effect of MOR and DOR agonists DAMGO and DADLE, which was manifested in control animals (group − M10), was not detected in morphine-adapted rats (group + M10). This result, demonstrated for basal as well as Forskolin-stimulated AC, supports the previously published data describing the decrease (desensitization) of G protein response to opioid stimulation in drug-addicted state [27–30,32] and is directly relevant and in agreement with principal finding of He and Whistler [57] indicating that chronic morphine resulted in a significant attenuation of the DAMGO-mediated inhibition of AC activity.

3.5. Increase in number of δ-opioid receptors (DOR)

In crude membrane preparations of monkey cortex and thalamus, the magnitude of MOR-, DOR- and KOR-stimulated G protein responses was proportional to the corresponding receptor densities

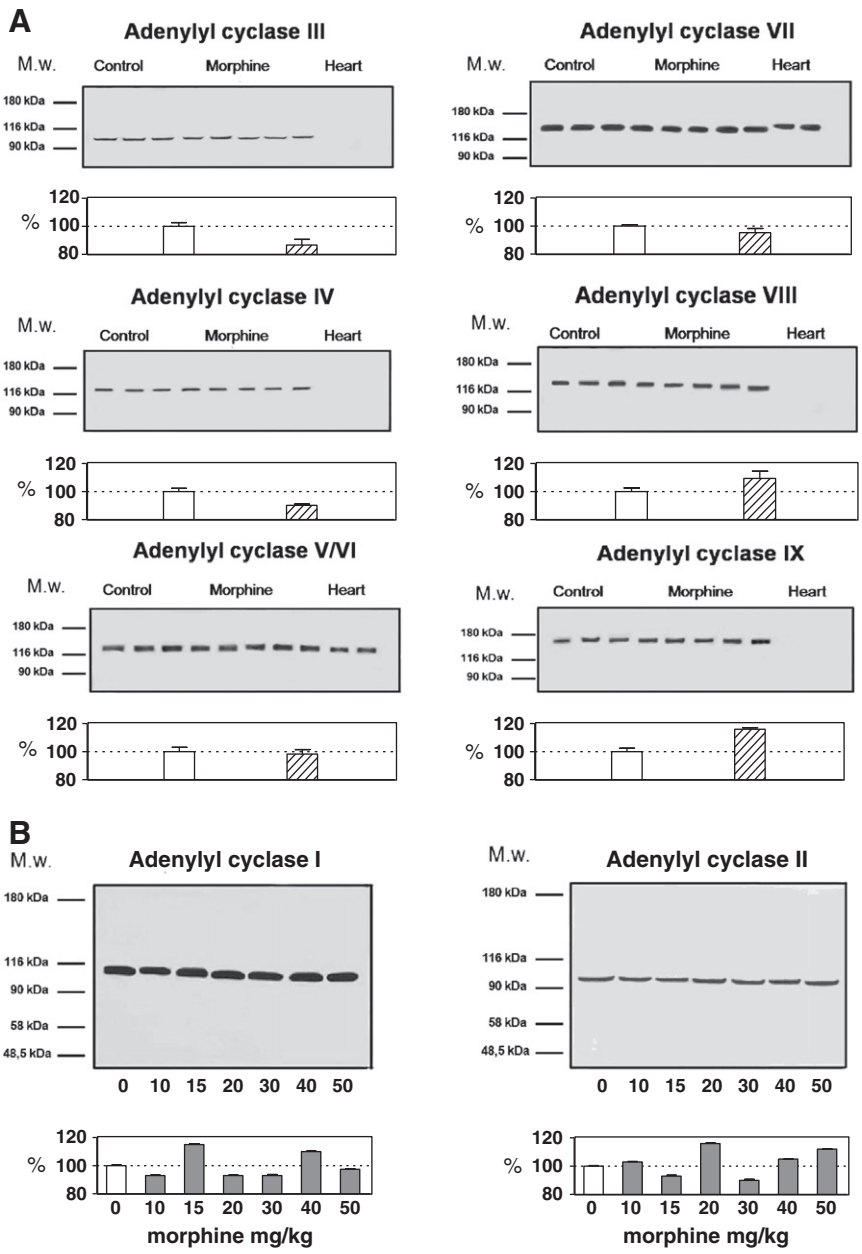

Fig. 2. Adenylyl cyclases III, IV, V/VI, VII, VIII and IX; *immunoblot analysis*. A. Membrane content of ACIII–IX was determined in PM isolated from brain cortex of morphine-adapted (group + M10) and control rats (group − M10) by quantitative immunoblotting. Typical immunoblots performed with the same amount of PM protein resolved in the same gel [4 × (− M10) plus 4 × (+ M10) samples] are shown. Statistical analysis was based on analysis of 3 immunoblots [4 × (− M10) plus 4 × (+ M10) samples in each gel/blot]. Numbers represent the average + M10/− M10 ratio ± SEM expressed as% of control (− M10) values, 100%. B. PM were isolated from animals exposed to the same doses of morphine (10, 15, 20, 30, 40 and 50 mg/kg) as in long-term adaptation experiment (Fig. 1), but for 24 h only (group + M1). Control animals were exposed to the single injection of PBS and sacrificed after 24 h (group − M1). As before, immunoblotting was performed with the same amount of PM protein resolved in the same gel [4 × (− M1) plus 4 × (+ M1). samples]. Both types of samples were run in parallel. Statistical analysis was based of comparison of (− M1) and (+ M1) samples in 3 immunoblots. Numbers represent the average + M1/− M1 ratio ± SEM expressed as% of control values, 100%.

[58]. Accordingly, the studies dealing with MOR in CHO cells [59] and in brain [60,61] indicated that the relationship between MOR occupancy and G protein activation depends on the receptor density [59–61]. As these studies were primarily oriented to MOR we decided to compare DOR density in PM prepared from control and morphine-adapted rat brain cortex.

DOR receptors in control (− M10) and morphine-treated (+ M10) brain cortex were characterized by saturation binding studies with DOR agonists [^{3}H]DADLE and [^{3}H]DPDPE. Saturation binding curves were measured in 0.1–34.4 nM ([^{3}H]DADLE) and 0.1–57.3 nM ([^{3}H] DPDPE) range of agonist concentrations in the presence or absence of 100 mM NaCl.

As shown in Fig. 6, maximum number of [^{3}H]DADLE binding sites in membranes isolated from morphine-adapted rats ($B_{max} = 0.115$ pmol . mg^{-1}) was 1.4× higher than in membranes isolated from control rats ($B_{max} = 0.083$ pmol . mg^{-1}). Surprisingly, 100 mM sodium chloride had no effect on [^{3}H]DADLE binding in morphine-adapted samples, but, as expected, it did inhibit radioligand binding to control membranes.

Morphine-induced increase of ligand binding to DOR was substantially higher when more specific ligand, [^{3}H] DPDPE, was

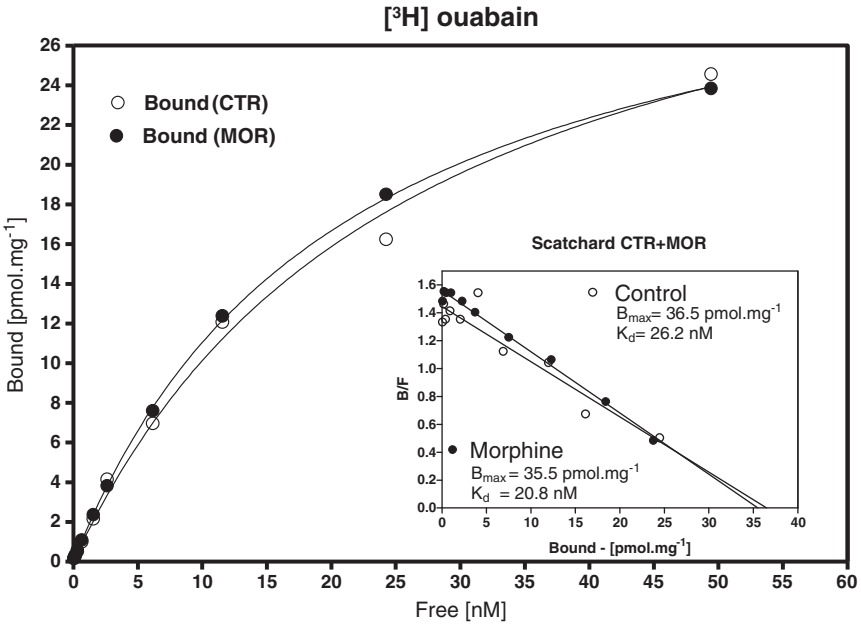

Fig. 3. Maximum binding capacity (B_{max}) and dissociation constant (K_d) of [^{3}H] ouabain binding sites in PM isolated from control and morphine-treated rats. Binding of selective Na, K-ATPase inhibitor [^{3}H] ouabain to PM isolated from brain cortex of control (−M10) and morphine-treated (+M10) rats was determined as described in Material and methods. Data were analyzed by GraphPad*Prism4*. B_{max} and K_d values represent the average of 3 experiments, each performed in triplicates.

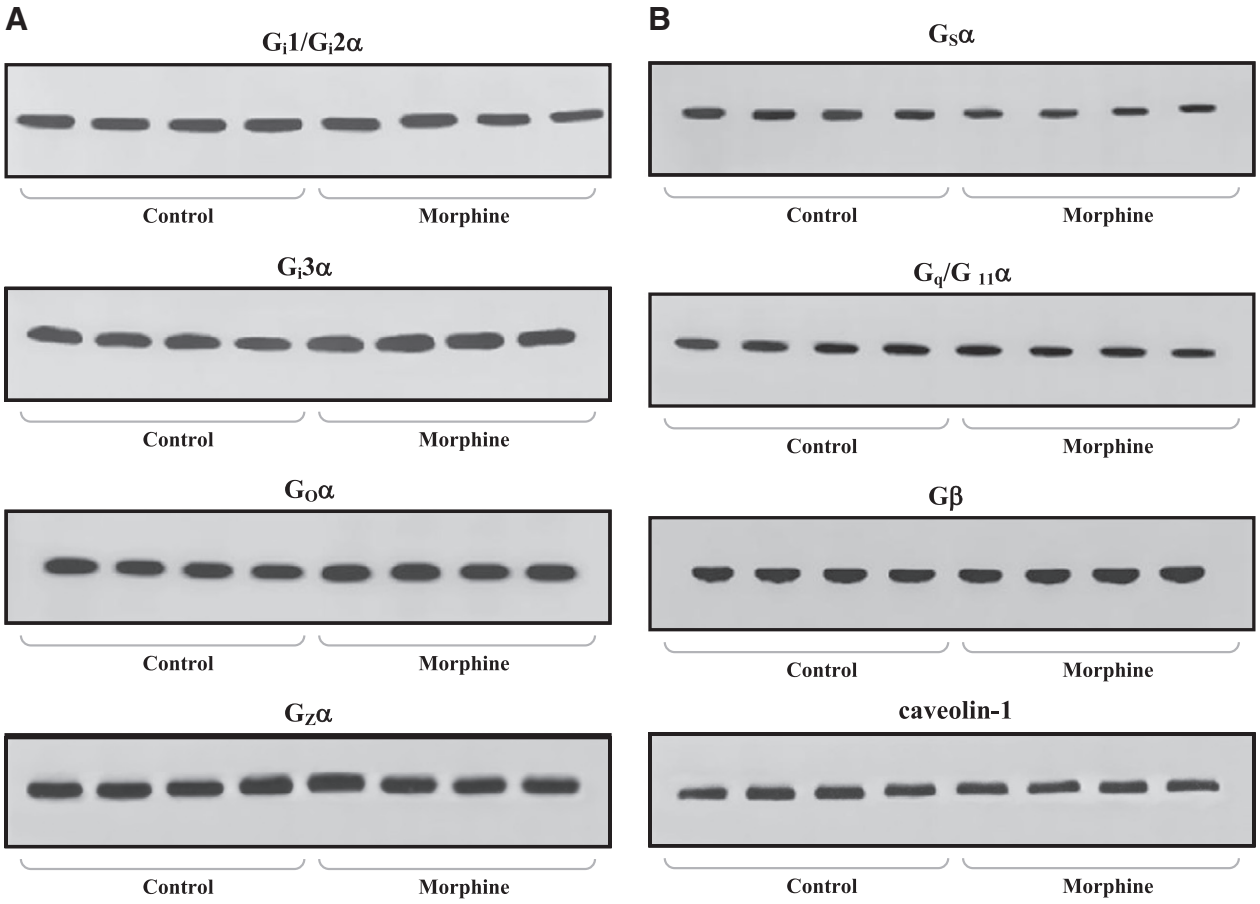

Fig. 4. Comparison of G protein content in PM isolated from control and morphine-adapted rats; $G_i1/G_i2\alpha$, $G_i3\alpha$, $G_z\alpha$, $G_s\alpha$, $G_q/G_{11}\alpha$, $G\beta$. PM protein (10 μg per well) was resolved by standard SDS-PAGE in Bio Rad Mini Protean II or by NuPAGE system (Invitrogen). G protein α and β subunits were identified by immunoblotting with specific antibodies as described in Material and methods. Caveolin-1 was determined as a marker of membrane domains. Data represent the typical immunoblots. $G_z\alpha$ and Gβ were resolved by NuPAGE electrophoretic system (Invitrogen); all other proteins were resolved by standard SDS-PAGE (BioRad). Statistical analysis was based on analysis of 3 immunoblots [4×(−M10) plus 4×(+M10) samples in each gel/blot]. Numbers represent the average + M10/−M10 ratio ± SEM expressed as% of control (−M10) values, 100%.

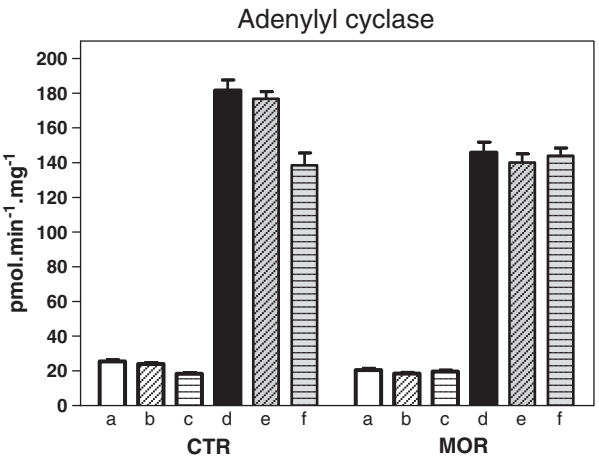

Fig. 5. Adenylyl cyclase enzyme activity. AC activity was measured in the absence (a, b, c) or presence of 10 μM Forskolin (d, e, f) in PM isolated from control (CTR, group − M10) or morphine-adapted (MOR, group + M10) rats as described in Material and methods. (a, d), basal activity, i.e. no additions; (b, e), 10 μM DADLE (δ-opioid agonist); (c, f), 10 μM DAMGO (μ-opioid agonist). Data represent the average of 3 experiments ± SEM.

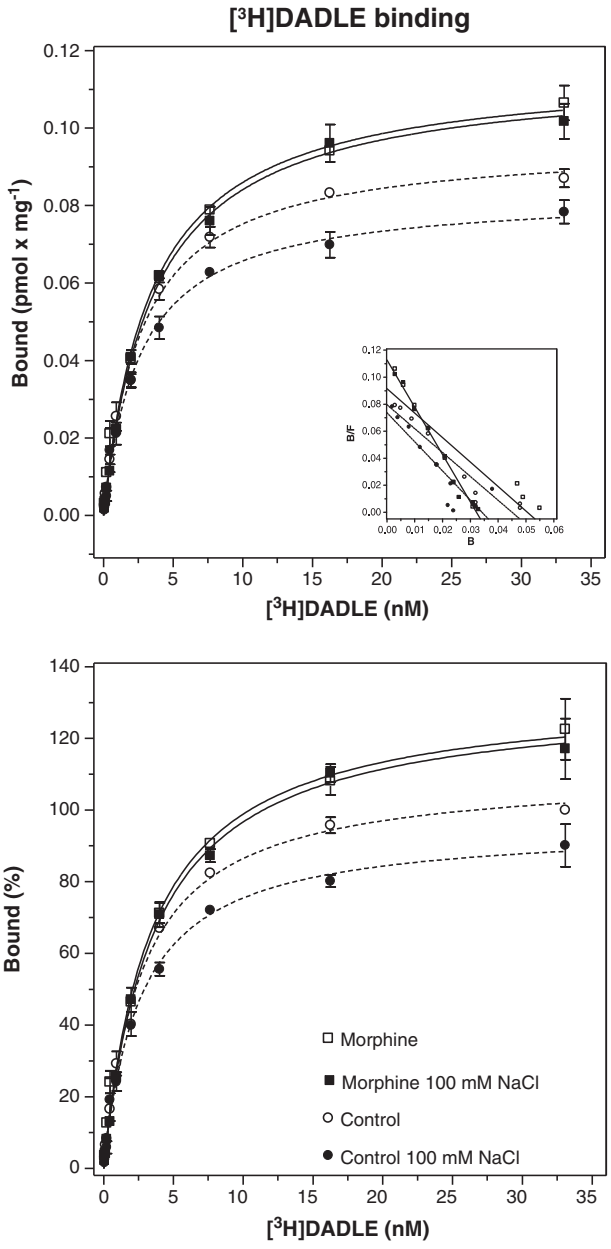

Fig. 6. Agonist binding characteristics of DOR; [^{3}H] DADLE. Saturation of specific [^{3}H] DADLE binding sites in control (− M10) and morphine-adapted (+ M10) plasma membrane samples was measured in 0.15–35 nM range of radioligand concentrations in the presence (+ NaCl) or absence (− NaCl) of 100 mM NaCl. The B_{max} and K_d values were calculated by GraphPad*Prizm4*. The data represent the average of three experiments performed in triplicates ± SEM. (○), controls, − NaCl; (●), controls, + NaCl; (□), morphine-adapted, − NaCl; (■), morphine-adapted, + NaCl.

used for determination of DOR in brain membranes. Maximum number of [^{3}H]DPDPE binding sites in morphine-treated membranes ($B_{max} = 0.057$ pmol . mg^{-1}) was 2.1× higher than in control ($B_{max} = 0.027$ pmol . mg^{-1}), Fig. 7. The effect of sodium chloride on [^{3}H]DPDPE binding was similar to that on [^{3}H]DADLE binding: inhibition was detected in control membranes only.

The difference between the two radioligands may be explained by higher specificity of [^{3}H]DPDPE to DOR in samples prepared from brain as the brain tissue contains, besides δ-opioid-receptors, high amount of μ- and κ-receptors [58]: maximum number of radioligand binding sites occupied by [^{3}H]DADLE was significantly higher than that recognized by [^{3}H]DPDPE. Therefore, morphine-induced increase of DOR detected by [^{3}H] DPDPE (2.1×) represents a "better estimate" of the actual increase of DOR density in PM isolated from morphine-adapted rats.

Sodium ions have been described as efficient inhibitors of agonist binding to numerous GPCR including OR causing the shift of receptor molecules towards the non-active state and uncoupling DOR from the cognate G protein, i.e. inverse agonist effect [62–65]. Sodium ions also decrease the basal GDP/GTP exchange of G_i/G_o proteins [66]. The low sensitivity of DOR to inhibitory effect of NaCl in morphine-adapted samples may be therefore interpreted as disturbance of equilibrium between active and non-active forms of receptor molecules.

4. Discussion

Opioid *addiction* has been long recognized as neurological disease involving the development of complex behavior characterized by drug tolerance, dependence and craving for the drug. The efforts to elucidate the molecular and cellular mechanisms of opioid *addiction* extend over many years and their results may be classified into two main hypotheses [1]:

(a) According to *homeostasis theory*, the drug disturbs cellular homeostasis and its effects are compensated by the activation of pathways that produce opposite effects and thus restore homeostasis.
(b) According to *desensitization theory*, the change of the drug–receptor interaction, receptor–G protein interaction or of some other, down-stream steps of OR-stimulated cascade renders the receptor less sensitive to the drug [1,7,57,67].

The *homeostasis* model involves an alteration of the amount of macromolecules in the cell, while the *desensitization* hypothesis does not because the negative change of drug–receptor interaction or subsequent steps of OR-initiated cascade may proceed with unchanged level of down-stream effectors. Our previous data [27] indicated that long-term adaptation of rats to increasing doses of morphine (according to the same protocol as that used in this work, group + M10) induces the *desensitization* of trimeric G protein response to MOR and DOR agonists (high-affinity GTPase and GTPγS binding assays). Desensitization of G protein response was demonstrated in plasma-membrane fraction isolated from rat brain cortex [27,40]. Furthermore, behavioral studies performed with the same group of animals indicated that these animals were fully "*drug*

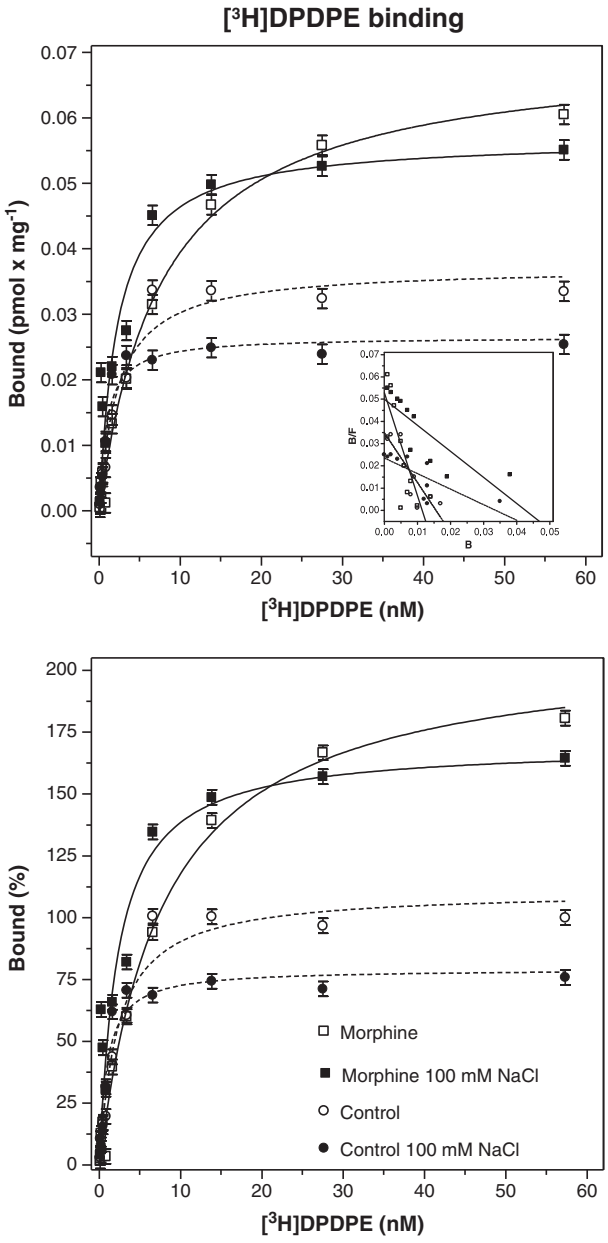

Fig. 7. Agonist binding characteristics of DOR; [^{3}H] DPDPE. Saturation of specific [^{3}H] DPDPE binding sites in control (−M10) and morphine-treated (+M10) plasma membrane samples was measured in 0.15–35 nM range of radioligand concentrations in the presence (+NaCl) or absence (−NaCl) of 100 mM NaCl. The B_{max} and K_d values were calculated by GraphPad*Prizm4*. The data represent the average of three experiments performed in triplicates ± SEM. (○), controls, −NaCl; (●), controls, +NaCl; (□), morphine-adapted, −NaCl; (■), morphine-adapted, +NaCl.

adapted" (*hot-plate* and *hind paw withdrawal* tests of tolerance). The state of *drug dependence* was also manifested by ptosis, chewing, diarrhea, increased sensitivity to touch and teeth clattering after drug withdrawal [27].

These results were fully compatible with data reported earlier by other authors who used auto-radiographic detection of the high-affinity [〈35〉S] GTPγS binding sites in different brain regions, mainly in specific areas of brain stem [28–30]. Thus, the decrease in functional response of G proteins persists in brain of animals fully adapted to morphine for prolonged period of time [27–30] and proceeds at the unchanged level of all the main classes of G proteins (Fig. 4). Accordingly, determination of AC activity in PM isolated from morphine-adapted rats indicated that inhibitory effect of opioid agonists, clearly manifested in control animals (group−M10), was *not* present in morphine-adapted rats (group+M10). This result has been demonstrated for basal as well as Forskolin-stimulated AC activity (Fig. 5) and was in full agreement with the data of He and Whistler [57].

Significance of the dramatic increase of ACI (8×) and ACII (2x) described in this work (Fig. 1A) was strongly supported by additional data indicating the specificity of this increase as the level of all other AC isoforms (AC III–IX) was unchanged (Fig. 2A) and that the increase of ACI and II was not detected in membranes exposed to the same doses of morphine, but for 24 h only (Fig. 2B).

It may be assumed that desensitization of G protein response for prolonged period of time (10 days) serves as an impulse for induction of compensatory response — proteosynthesis leading to specific increase of ACI and II in PM of morphine-adapted rats. This interpretation is fully in line with characteristics of molecular mechanisms of opioid tolerance and addiction as an example for homeostatic control aiming to keep the performance of target cell metabolism at unchanged level [1]. Finally, after withdrawal of the drug for 20 days, AC levels return back to the normal state (Fig. 1B).

Data presented in this work thus fall in line between the two above mentioned hypotheses of drug addiction as homeostatic mechanisms and activation of specific proteosynthetic pathways are obviously responsible for increase in plasma membrane density of ACI and ACII, simultaneously, the decrease of G protein response to OR stimulation detected in the same type of membranes [27], may be regarded as a part of desensitization mechanism of morphine action.

In brain, ACI and ACII represent the highly expressed and physiologically important species of this crucial regulatory enzyme of cAMP-dependent signaling cascades [31,68–70]. Sensitization, activation or over-shoot of AC activity after prolonged exposure of cultured cells or brain tissue to morphine has been demonstrated in previous studies of mechanism of action of this drug [1,7,8,16–23,26]. These data, however, were up to now not accompanied by the detailed analysis of the individual subtypes of AC protein molecules in plasma membranes isolated from brain cortex. Furthermore, the efforts to explain the molecular mechanism of the increase of AC activity by long-term morphine treatment have not so far resulted in a commonly accepted interpretation as widely different and even contradictory results were obtained [1,7,21,22,28,29,57].

The increase of ACI and II which has been clearly demonstrated in this work has to be considered together with the unchanged level of all other types of AC molecules and PM markers Na,K-ATPase, trimeric G protein subunits and caveolin-1. The unchanged level of these PM proteins brings strong evidence for the *specificity* of the long-term morphine effect on ACI and II. *Therefore, data presented in this work bring new and original evidence which so far has not been presented in the up-to-date literature and help for better understanding of the complicated pathological phenomenon denominated as drug addiction.*

We suggest that the positive as well as negative regulatory circuits exist at different steps of OR-induced signaling pathways when responding to prolonged exposure to morphine in the course of full adaptation to this drug. Decrease of G protein response to OR stimulation, *desensitization*, persists in animals adapted to morphine for 10- or 12 days [27–30], while the levels of all the main classes of G proteins remained unchanged (Fig. 4). Consequently, the decrease in inhibitory effect of G proteins on AC activity was measured in PM isolated from morphine-adapted rats (Fig. 5). It may be therefore assumed that the synthesis of new ACI and II molecules represents the *specific*, compensatory response leading to the increased plasma membrane density of these protein molecules (Fig. 1A, left panels).

Our results and interpretation are also relevant to analysis of drug tolerance and addiction states of mammalian organism as behavioral tests performed under in vivo conditions indicated that morphine-adapted animals have been fully *drug dependent* and developed *tolerance* to subsequent drug addiction [27].

Explanation why ACI and ACII differ when responding to the long-term morphine treatment can hardly be clear-cut and unequivocal as these two isoforms differ substantially when responding to different GPCR agonists and activated forms of G proteins [25,68–70]. ACI is known to be inhibited by free $G_o\alpha$ and $G\beta\gamma$ subunits [10,68,70], while ACII activity is dramatically activated/potentiated by $G\beta\gamma$ in the presence free $G_s\alpha$ subunits [21,22,25,69]. Nevertheless, we assume that the decreased response of PTX-sensitive G proteins of G_i/G_o family to MOR and DOR agonists in morphine-adapted rats (desensitization) represents the primary impulse for subsequent compensatory response increasing the expression level of ACI and II. Preferential increase of ACI (Fig. 1A) and attenuation of DAMGO-mediated inhibition of AC activity (Fig. 5) [57] suggests the primary involvement of "classical, inhibitory pathway" proceeding via MOR and inhibition of ACI activity [68,70].

5. Conclusions

Data presented in this work extend the knowledge and bring more close view to understanding of the long-term adaptation of mammalian organism to morphine and widely studied phenomena of drug addiction and tolerance.

We have found that:

- plasma membrane density of ACI and II molecules was increased largely and this increase was disproportionate between ACI (8×) and ACII (2.5×) in rats adapted to increasing doses of morphine for prolonged period of time, 10 days,
- increase of ACI and II represented the specific effect as the level of ACIII–IX was unchanged,
- levels of plasma membrane marker Na, K-ATPase and caveolin-1 were unchanged,
- membrane density of all the major classes of trimeric G proteins was unchanged;
- number of δ-opioid receptors was increased 2× and agonist binding to these receptor sites was not affected by sodium ions;
- difference in responsiveness of different AC isoforms to the long-term morphine treatment may be interpreted as preferential activation of specific synthetic pathway leading to production of new ACI and AC II molecules,
- increase of ACI and II was not detected in PM prepared from rats exposed to the same doses of morphine, but for 24 h only (short-term exposure),
- analysis of PM isolated from animals adapted to morphine for 10 days and subsequently nurtured for 20 days in the absence of the drug indicated that membrane density of both ACI and ACII returned fully to the control level observed in morphine-unexposed rats. *Thus, the major reorganization of the complement of AC molecules in plasma membrane, arising as a compensatory response to the long-term adaptation to morphine, was fully reversible.*

Acknowledgements

This work was supported by projects LC554 and LC06063 of MSMT, GACR (305/08/H037) and the Academy of Sciences of the Czech Republic (AV0Z50110509). The authors thank Ing. Martin Chmatal, CSc and Bc. Katerina Kasparovska for performing [^{3}H]ouabain binding assays and valuable help.

References

[1] P.Y. Law, H.H. Loh, L.N. Wei, Insights into the receptor transcription and signaling: implications in opioid tolerance and dependence, Neuropharmacology 47 (2004) 300–311.
[2] C.J. Evans, D.E. Keith, H. Morrison Jr., K. Magendzo, R.H. Edwards, Cloning of a delta opioid receptor by functional expression, Science 258 (1992) 1952–1955.
[3] B.L. Kieffer, K. Befort, C. Gaveriaux-Ruff, C.G. Hirth, The delta-opioid receptor: isolation of a cDNA by expression cloning and pharmacological characterization, Proc. Natl. Acad. Sci. U. S. A. 89 (1992) 12048–12052.
[4] B.L. Kieffer, Opioids: first lessons from knockout mice, Trends Pharmacol. Sci. 20 (1999) 19–26.
[5] Y. Chen, A. Mestek, J. Liu, J.A. Hurley, L. Yu, Molecular cloning and functional expression of a mu-opioid receptor from rat brain, Mol. Pharmacol. 44 (1993) 8–12.
[6] Y. Chen, A. Mestek, J. Liu, L. Yu, Molecular cloning of a rat kappa opioid receptor reveals sequence similarities to the mu and delta opioid receptors, Biochem. J. 295 (1993) 625–628.
[7] J.L. Whistler, M. von Zastrow, Morphine-activated opioid receptors elude desensitization by beta-arrestin, Proc. Natl. Acad. Sci. U. S. A. 95 (1998) 9914–9919.
[8] J.L. Whistler, H.H. Chuang, P. Chu, L.Y. Jan, M. von Zastrow, Functional dissociation of μ-opioid receptor signaling and receptor endocytosis: implications for the biology of opiate tolerance and addiction, Neuron 23 (1999) 737–746.
[9] C. Contet, B.L. Kieffer, K. Befort, Mu opioid receptor: a gateway to drug addiction, Curr. Opin. Neurobiol. 14 (2004) 370–378.
[10] B.D. Carter, F. Medzihradsky, Go mediates the coupling of the mu opioid receptor to adenylyl cyclase in cloned neural cells and brain, Proc. Natl. Acad. Sci. U.S.A. 90 (1993) 4062–4066.
[11] P. Gierschik, G. Milligan, M. Pines, P. Goldsmith, J. Codina, W. Klee, A. Spiegel, Use of specific antibodies to quantitate the guanine nucleotide-binding protein Go in brain, Proc. Natl. Acad. Sci. U. S. A. 83 (1986) 2258–2262.
[12] P. Goldsmith, P. Gierschik, G. Milligan, C.G. Unson, R. Vinitsky, H.L. Malech, A.M. Spiegel, Antibodies directed against synthetic peptides distinguish between GTP-binding proteins in neutrophil and brain, J. Biol. Chem. 262 (1987) 14683–14688.
[13] P.S. Backlund Jr., R.R. Aksamit, C.G. Unson, P. Goldsmith, A.M. Spiegel, G. Milligan, Immunochemical and electrophoretic characterization of the major pertussis toxin substrate of the RAW264 macrophage cell line, Biochemistry 27 (1988) 2040–2046.
[14] G. Milligan, Techniques used in the identification and analysis of function of pertussis toxin-sensitive guanine nucleotide binding proteins, Biochem. J. 255 (1988) 1–13.
[15] G. Milligan, Immunological probes and the identification of guanine nucleotide-binding proteins, in: M.D. Houslay, G. Milligan (Eds.), G proteins as Mediators of Cellular Signaling Processes, John Wiley & Sons. Ltd., New York, 1990, pp. 31–46.
[16] S.K. Sharma, M. Nierenberg, W.A. Klee, Morphine receptors as regulators of adenylate cyclase activity, Proc. Natl. Acad. Sci. U. S. A. 72 (1975) 590–594.
[17] S.K. Sharma, W.A. Klee, M. Nierenberg, Dual regulation of adenylate cyclase accounts for narcotic dependence and tolerance, Proc. Natl. Acad. Sci. U.S.A. 72 (1975) 3092–3096.
[18] B. Attali, Z. Vogel, Long-term opiate exposure leads to reduction of the alpha i-1 subunit of GTP-binding proteins, J. Neurochem. 53 (1989) 1636–1639.
[19] T. Avidor-Reiss, M. Baywatch, R. Levy, N. Matus-Leibovitch, I. Nevo, Z. Vogel, Adenylylcyclase super-sensitization in mu-opioid receptor-transfected Chinese hamster ovary cells following chronic opioid treatment, J. Biol. Chem. 270 (1995) 29732–29738.
[20] T. Avidor-Reiss, I. Nevo, R. Levy, T. Pfeuffer, Z. Vogel, Chronic opioid treatment induces adenylyl cyclase V superactivation. Involvement of Gβγ, J. Biol. Chem. 271 (1996) 21309–21315.
[21] H. Ammer, R. Schulz, Enhanced stimulatory adenylyl cyclase signaling during opioid dependence is associated with a reduction in palmitoylated Gs alpha, Mol. Pharmacol. 52 (1997) 993–999.
[22] H. Ammer, R. Schulz, Adenylyl cyclase super-sensitivity in opioid-withdrawn NG108-115 hybrid cells requires Gs but is not mediated by Gs alpha subunit, J. Pharmacol. Exp. Ther. 286 (1998) 855–862.
[23] M.L. Bayewitch, I. Nevo, T. Avidor-Reiss, R. Levy, W.F. Simonds, Z. Vogel, Alterations in detergent solubility of heterotrimeric G proteins after chronic activation of G(i/o)-coupled receptors: changes in detergent solubility are in correlation with onset of adenylyl cyclase superactivation, Mol. Pharmacol. 57 (2000) 820–825.
[24] H. Ammer, T.E. Christ, Identity of adenylyl cyclase isoform determines the G protein mediating chronic opioid-induced adenylyl cyclase supersensitivity, J. Neurochem. 83 (2002) 818–827.
[25] P.H. Tso, Y.H. Wong, Molecular basis of opioid dependence: role of signal regulation by G-proteins, Clin. Exp. Pharmacol. Physiol. 30 (2003) 307–316.
[26] E. Schallmach, D. Steiner, Z. Vogel, Adenylyl cyclase type II activity is regulated by two different mechanisms: implications for acute and opioid exposure, Neuropharmacology 50 (2006) 998–1005.
[27] L. Bourova, M. Vosahlikova, D. Kagan, K. Dlouha, J. Novotny, P. Svoboda, Long-term adaptation to high doses of morphine causes desensitization of μ-OR- and δ-OR-stimulated G protein response in forebrain cortex but not the decrease in the amount of G protein alpha subunits, Med. Sci. Monit. 16 (2010) BR260–BR270.
[28] L.J. Sim, D.E. Selley, S.I. Dworkin, S.R. Childers, Effects of chronic morphine administration on mu opioid receptor-stimulated [^{35}S] GTPgammaS autoradiography in rat brain, J. Neurosci. 16 (1996) 2684–2692.
[29] L.J. Sim-Selley, D.E. Selley, L.J. Vogt, S.R. Childers, T.J. Martin, Chronic heroin self-administration desensitizes mu opioid receptor-activated G-proteins in specific regions of rat brain, J. Neurosci. 20 (2000) 4555–4562.
[30] C.E. Maher, T.J. Martin, S.R. Childers, Mechanisms of mu opioid receptor/G-protein desensitization in brain by chronic heroin administration, Life Sci. 77 (2005) 1140–1154.
[31] C. Sanabra, G. Mengod, Neuroanatomical distribution and neurochemical characterization of cells expressing adenylyl cyclase isoforms in mouse and rat brain, J. Chem. Neuroanat. 41 (2011) 43–54.
[32] F.M. Mitchell, S.L. Griffiths, E.D. Saggerson, M.D. Houslay, J.T. Knowler, G. Milligan, Guanine-nucleotide-binding proteins expressed in rat white adipose tissue.

Identification of both mRNAs and proteins corresponding to Gi1, Gi2 and Gi3, Biochem. J. 262 (1989) 403–408.
[33] F.M. Mitchell, I. Mullaney, P.P. Godfrey, S.J. Arkinstall, M.J. Wakelam, G. Milligan, Widespread distribution of Gq alpha/G11 alpha detected immunologically by an antipeptide antiserum directed against the predicted C-terminal decapeptide, FEBS Lett. 287 (1991) 171–174.
[34] I. Mullaney, G. Milligan, Identification of two distinct isoforms of the guanine nucleotide binding protein Go in neuroblastoma × glioma hybrid cells: independent regulation during cyclic AMP-induced differentiation, J. Neurochem. 55 (1990) 1890–1898.
[35] I. Mullaney, M.W. Dodd, N. Buckley, G. Milligan, Agonist activation of transfected human M1 muscarinic acetylcholine receptors in CHO cells results in down-regulation of both the receptor and the alpha subunit of the G protein Gq, Biochem. J. 289 (1993) 125–131.
[36] I. Mullaney, F.M. Mitchell, J.F. McCallum, N.J. Buckley, G. Milligan, The human muscarinic M1 acetylcholine receptor when expressed in CHO cells, activates and down-regulates both Gq and G11 alpha equally and non-selectively, FEBS Lett. 324 (1993) 241–245.
[37] I. Mullaney, M.P. Caulfield, P. Svoboda, G. Milligan, Activation, cellular redistribution and enhanced degradation of the G proteins Gq and G11 by endogenously expressed and transfected phospholipase C-coupled muscarinic m1 acetylcholine receptors, Prog. Brain Res. 109 (1996) 181–187.
[38] I. Ihnatovych, J. Novotny, R. Haugvicova, L. Bourova, P. Mares, P. Svoboda, Ontogenetic development of G protein-mediated adenylyl cyclase signaling in rat brain, Brain Res. Dev. Brain Res. 133 (2002) 69–75.
[39] W.E. Evans, R.L. Coyer, M.F. Sandusky, M.J. Van Fleet, J.G. Moore, E. Nyquist, Characterization of membrane rats isolated from rat Sertoli cultures: caveolin and flotilin-1 content, J. Androl. 24 (2003) 812–821.
[40] L. Bourova, J. Stohr, V. Lisy, V. Rudajev, J. Novotny, P. Svoboda, Isolation of plasma membrane compartments from rat brain cortex; detection of agonist-stimulated G protein activity, Med. Sci. Monit. 15 (2009) BR111–BR122.
[41] Z. Moravcova, V. Rudajev, J. Stohr, J. Novotny, J. Cerny, M. Parenti, G. Milligan, P. Svoboda, Long-term agonist stimulation of IP prostanoid receptor depletes the cognate G(s)alpha protein in membrane domains but does not change the receptor level, Biochim. Biophys. Acta 1691 (2004) 51–65.
[42] P. Matousek, J. Novotny, P. Svoboda, Resolution of G(s)alpha and G(q)alpha/G (11)alpha proteins in membrane domains by two-dimensional electrophoresis: the effect of long-term agonist stimulation, Physiol. Res. 53 (2004) 295–303.
[43] P. Matousek, J. Novotny, V. Rudajev, P. Svoboda, Prolonged agonist stimulation does not alter the protein composition of membrane domains in spite of dramatic changes induced in a specific signaling cascade, Cell Biochem. Biophys. 42 (2005) 21–40.
[44] P. Svoboda, E. Amler, J. Teisinger, Different sensitivity of ATP + Mg + Na (I) and Pi + Mg (II) dependent types of oubain binding to phospholipase A2, J. Membr. Biol. 104 (1988) 211–221.
[45] L. Bourova, A. Kostrnova, L. Hejnova, Z. Moravcova, H.E. Moon, J. Novotny, G. Milligan, P. Svoboda, δ-opioid receptors exhibit high efficiency when activating trimeric G proteins in membrane domains, J. Neurochem. 85 (2003) 34–49.
[46] Y. Salomon, C. Londos, M. Rodbell, A highly sensitive adenylyl cyclase assay, Anal. Biochem. 58 (1974) 541–548.
[47] A.A. White, Separation and purification of cyclic nucleotides by alumina column chromatography, in: J.G. Hardman, B.W. O'Malley (Eds.), Methods in Enzymology, vol. 38C, Academic Press, 1974, pp. 41–46.
[48] H.E. Moon, A. Cavalli, D.S. Bahia, M. Hoffmann, D. Massotte, G. Milligan, The human δ opioid receptor activates Gi1α more efficiently than Go1α, J. Neurochem. 76 (2001) 1805–1813.
[49] G. Milligan, A. Green, Agonist control of G-protein levels, Trends Pharmacol. Sci. 12 (1991) 207–209.
[50] G. Milligan, Agonist regulation of cellular G protein levels and distribution: mechanisms and functional implications, Trends Pharmacol. Sci. 14 (1993) 413–418.
[51] F.M. Mitchell, N.J. Buckley, G. Milligan, Enhanced degradation of the phosphoinositidase C-linked guanine-nucleotide-binding protein Gq/G11 alpha following activation of the human M1 muscarinic acetylcholine receptor expressed in CHO cells, Biochem. J. 293 (1993) 495–499.
[52] F.R. McKenzie, G. Milligan, Prostaglandin E1-mediated, cyclic AMP-dependent down-regulation of Gs alpha in neuroblastoma × glioma hybrid cells, J. Biol. Chem. 265 (1990) 17084–17093.
[53] I. Mullaney, B.H. Shah, A. Wise, G. Milligan, Expression of the human β2-adrenoceptor in NCB20 cells results in agonist activation of adenylyl cyclase and agonist-mediated selective down-regulation of Gsα, J. Neurochem. 65 (1995) 545–553.
[54] P. Svoboda, L. Unelius, B. Cannon, J. Nedergaard, Attenuation of Gs alpha coupling efficiency in brown-adipose-tissue plasma membranes from cold-acclimated hamsters, Biochem. J. 295 (1993) 655–661.
[55] P. Svoboda, G.D. Kim, M.A. Grassie, K.A. Eidne, G. Milligan, Thyrotropin-releasing hormone-induced subcellular redistribution and down-regulation of G11 alpha: analysis of agonist regulation of co-expressed G11 alpha species variants, Mol. Pharmacol. 49 (1996) 646–655.
[56] P. Svoboda, L. Unelius, A. Dicker, B. Cannon, G. Milligan, J. Nedergaard, Cold-induced reduction in Gi alpha proteins in brown adipose tissue. Effects on the cellular hypersensitization to noradrenaline caused by pertussis-toxin treatment, Biochem. J. 314 (1996) 761–768.
[57] L. He, J.L. Whistler, The biochemical analysis of methadone modulation on morphine-induced tolerance and dependence in brain, Pharmacology 79 (2007) 193–202.
[58] M.C. Ko, H. Lee, C. Harrison, M.J. Clark, H.F. Song, N.N. Naughton, J.H. Woods, J.R. Traynor, Studies of mu-, kappa-, and delta-opioid receptor density and G protein activation in the cortex and thalamus of monkeys, J. Pharmacol. Exp. Ther. 306 (2003) 179–186.
[59] D.E. Selley, Q. Liu, S.R. Childers, Signal transduction correlates of mu opioid agonist intrinsic efficacy: receptor-stimulated [^{35}S]GTP gamma S binding in mMOR-CHO cells and rat thalamus, J. Pharmacol. Exp. Ther. 285 (1998) 496–505.
[60] L.J. Sim-Selley, J.B. Daunais, L.J. Porrino, S.R. Childers, Mu and kapp a1 opioid-stimulated [^{35}S]guanylyl-5′-O-(gamma-thio)-triphosphate binding in cynomolgus monkey brain, Neuroscience 94 (1999) 651–662.
[61] C.E. Maher, D.E. Selley, S.R. Childers, Relationship of mu opioid receptor binding to activation of G-proteins in specific rat brain regions, Biochem. Pharmacol. 59 (2000) 1395–1401.
[62] C.B. Pert, S.H. Snyder, Opiate receptor binding of agonists and antagonists affected differentially by sodium, Mol. Pharmacol. 10 (1974) 868–879.
[63] G. Koski, R.A. Streaty, W.A. Klee, Modulation of sodium-sensitive GTPase by partial opiate agonists. An explanation for the dual requirement for Na+ and GTP in inhibitory regulation of adenylate cyclase, J. Biol. Chem. 257 (1982) 14035–14040.
[64] H. Kong, K. Raynor, K. Yasuda, G.I. Bell, T. Reisine, Mutation of aspartate at residue 89 in somatostatine receptor subtype 2 prevents Na+ regulation of agonist binding but does not alter receptor–G protein interaction, Mol. Pharmacol. 44 (1993) 380–384.
[65] H. Kong, K. Raynor, K. Yasuda, S.T. Moe, P.S. Portoghese, G.I. Bell, T. Reisine, A single residue, aspartic acid 95, in the δ-opioid receptor specifies selective high affinity agonist binding, J. Biol. Chem. 268 (1993) 23055–23058.
[66] R. Seifert, K. Wenzel-Seifert, Constitutive activity of G-protein coupled receptors: cause of disease and common property of wild-type receptors, Naunyn-Schmiedeberg's Arch. Pharmacol. 366 (2002) 381–416.
[67] L. He, J.L. Whistler, An opiate cocktail that reduces morphine tolerance and dependence, Curr. Biol. 15 (2005) 1028–1033.
[68] J. Hanoune, N. Defer, Regulation and role of adenylyl cyclase isoforms, Annu. Rev. Pharmacol. Toxicol. 41 (2001) 145–174.
[69] R.K. Sunahara, R. Taussig, Isoforms of mammalian adenylyl cyclase: multiplicities of signaling, Mol. Interv. 2 (2002) 168–184.
[70] T.B. Patel, Z. Du, S. Pierre, L. Cartin, K. Scholich, Molecular biological approaches to unravel adenylyl cyclase signaling and function, Gene 269 (2001) 13–25.

Ujcikova et al. Proteome Science 2014, 12:11
http://www.proteomesci.com/content/12/1/11

PROTEOME SCIENCE

RESEARCH Open Access

Proteomic analysis of post-nuclear supernatant fraction and percoll-purified membranes prepared from brain cortex of rats exposed to increasing doses of morphine

Hana Ujcikova[1], Adam Eckhardt[2], Dmytro Kagan[1], Lenka Roubalova[1] and Petr Svoboda[1*]

Abstract

Background: Proteomic analysis was performed in post-nuclear supernatant (PNS) and Percoll-purified membranes (PM) prepared from fore brain cortex of rats exposed to increasing doses of morphine (10–50 mg/kg) for 10 days.

Results: In PNS, the 10 up (↑)- or down (↓)-regulated proteins exhibiting the *largest morphine-induced change* were selected, excised manually from the gel and identified by MALDI-TOF MS/MS: **1**-(gi|148747414, Guanine deaminase), ↑2.5×; **2**-(gi|17105370, Vacuolar-type proton ATP subunit B, brain isoform), ↑2.6×; **3**-(gi|1352384, Protein disulfide-isomerase A3), ↑3.4×; **4**-(gi|40254595, Dihydropyrimidinase-related protein 2), ↑3.6×; **5**-(gi|149054470, N-ethylmaleimide sensitive fusion protein, isoform CRAa), ↑2.0×; **6**-(gi|42476181, Malate dehydrogenase, mitochondrial precursor), ↑1.4×; **7**-(gi|62653546, Glyceraldehyde-3-phosphate dehydrogenase), ↑1.6×; **8**-(gi|202837, Aldolase A), ↑1.3×; **9**-(gi|31542401, Creatine kinase B-type), ↓0.86×; **10**-(gi|40538860, Aconitate hydratase, mitochondrial precursor), ↑1.3×. The identified proteins were of cytoplasmic (**1, 4, 5, 7, 9**), cell membrane (**2**), endoplasmic reticulum (**3**) and mitochondrial (**6, 8, 10**) origin and 9 of them were significantly increased, 1.3-3.6×. The 4 out of 9 up-regulated proteins (**4, 6, 7, 10**) were described as functionally related to oxidative stress; the 2 proteins participate in genesis of apoptotic cell death.
In PM, the 18 up (↑)- or down (↓)-regulated proteins were identified by LC-MS/MS and were of *plasma membrane* [Brain acid soluble protein, ↓2.1×; trimeric Gβ subunit, ↓2.0x], *myelin membrane* [MBP, ↓2.5×], *cytoplasmic* [Internexin, ↑5.2×; DPYL2, ↑4.9×; Ubiquitin hydrolase, ↓2.0×; 60S ribosomal protein, ↑2.7×; KCRB, ↓2.6×; Sirtuin-2, ↑2.5×; Peroxiredoxin-2, ↑2.2×; Septin-11, ↑2.2×; TERA, ↑2.1×; SYUA, ↑2.0×; Coronin-1A, ↓5.4×] and *mitochondrial* [Glutamate dehydrogenase 1, ↑2.7×; SCOT1, ↑2.2×; Prohibitin, ↑2.2×; Aspartate aminotransferase, ↓2.2×] origin. Surprisingly, the immunoblot analysis of the same PM resolved by 2D-ELFO indicated that the "active", morphine-induced pool of Gβ subunits represented just a minor fraction of the total signal of Gβ which was decreased 1.2x only. The dominant signal of Gβ was unchanged.

Conclusion: Brain cortex of rats exposed to increasing doses of morphine is far from being adapted. Significant up-regulation of proteins functionally related to oxidative stress and apoptosis suggests a major change of energy metabolism resulting in the state of severe brain cell "discomfort" or even death.

Keywords: Morphine, Long-term adaptation, Fore brain cortex, Isolated plasma membranes, Post-nuclear supernatant, 2D electrophoresis

* Correspondence: svobodap@biomed.cas.cz
[1]Laboratories of Biochemistry of Membrane Receptors, Institute of Physiology, v.v.i., Academy of Sciences of the Czech Republic, Videnska 1083, Prague 4 14220, Czech Republic
Full list of author information is available at the end of the article

Background

Morphine is one of the most effective painkillers. Repeated exposure of experimental animals to morphine results in tolerance to this drug, development of physical dependence and a chronic relapsing disorder – drug addiction [1-5]. Physical dependence contributes to a drug seeking behavior and the continuous drug use with the aim to prevent the onset of unpleasant withdrawal symptoms. To name just few, morphine-induced changes of brain function were associated with alternations of synaptic connectivity [6], neurotransmission [7], specific signaling cascades [8], energy metabolism [9] and stability of protein molecules [10].

Hyper-sensitization or super-activation of adenyl cyclase (AC) activity by prolonged exposure of cultured cells or mammalian organism to morphine has been demonstrated in previous studies of mechanism of action of this drug [1-5] and considered as biochemical basis for development of opiate *tolerance* and *dependence*.

Our previous work on isolated Percoll® membranes (PM) prepared from brain cortex of rats exposed to morphine for 10 days (10–50 mg/kg) indicated a desensitization of G-protein response to μ-OR (DAMGO) and δ-OR (DADLE) stimulation [11] and specific increase of ACI (8x) and ACII (2.5×) isoforms [12]. The κ-OR (U-23554)-stimulated [^{35}S] GTPγS binding and expression level of ACIII-IX in PM was unchanged. Behavioral tests of morphine-treated animals indicated that these animals were fully drug-dependent (opiate abstinence syndrome) and developed tolerance to subsequent drug addition (analgesic tolerance - hot-plate and hind paw withdrawal tests). The increase of ACI and ACII was interpreted as a specific compensatory response to prolonged stimulation of brain cortex OR by morphine.

Proteomic analysis represents a useful approach for an investigation of the overall changes of protein composition induced by the short-term or prolonged use of drugs. The aim of our present work was to identify proteins which are significantly altered in brain cortex of rats exposed to the increasing, high doses of morphine for prolonged period of time (10 days). For this aim, the post-nuclear supernatant fraction (PNS) was analyzed because it contains proteins of mitochondrial, endoplasmic reticulum, plasma membrane as well as cytoplasmic origin. In the second part of our work, we extended these studies by analysis of protein composition in membrane fraction isolated in Percoll gradient (PM).

Results

Two-dimensional electrophoresis and protein identification in post-nuclear supernatant prepared from brain cortex of control and morphine-treated rats; *analysis by MALDI-TOF MS/MS*

Samples of PNS were extracted in ice-cold aceton/TCA/96% ethanol, resolved by 2D-ELFO in linear IPG strips (pH 3–11) and 10% w/v acrylamide/0.26% w/v bis-acrylamide gels as described in methods and stained with silver or colloidal Coomassie blue. The stained 2D gels were scanned with an imaging densitometer and quantified by PDQuest software.

About 440 protein spots were recognized by silver staining and PDQuest analysis of gels in both types of PNS (Figure 1, left panels); when stained in colloidal Coomassie blue, about 200 spots were recognized. In CBB-stained gels, proteins 1–10 with different mobility in (+M10) and (−M10) samples were selected for identification by MALDI-TOF MS/MS as described in methods (Figure 1, right panels). The detailed list of the altered and identified proteins is presented in Additional file 1: Table S1 and Table 1. These tables also include description of the subcellular localization and function of these proteins.

The identified proteins were of cytoplasmic (**1**-Guanine deaminase, ↑2.5×; **4**-Dihydropyrimidinase-related protein 2,↑3.6×; **5**-N-ethylmaleimide sensitive fusion protein, isoform CRAa, ↑2.0×; **7**-Glyceraldehyde-3-phosphate dehydrogenase, ↑1.6×; **9**-Creatine kinase B-type, ↓0.86), cell membrane (**2**-Vacuolar-type proton ATPase, subunit B, brain isoform), ↑2.6x), endoplasmic reticulum (**3**-Protein disulfide-isomerase A3, ↑3.4×) and mitochondrial (**6**-Malate dehydrogenase, mitochondrial precursor, ↑1.4x; **8**-Aldolase A, ↑1.3×; **10**-Aconitate hydratase, mitochondrial precursor, ↑1.3x) origin. The 9 of them were significantly increased, 1.3-3.6x. Correlation with functional properties of these proteins indicated up-regulation of proteins related to guanine degradation (**1**), vacuolar acidification (**2**), apoptotic cell death (**3**), oxidative stress (**4, 6, 7, 10**), membrane traffic (**5**) and glycolysis (**8**). All together, the spectrum of the altered proteins suggests a major alternation of brain cortex tissue when exposed to increasing doses of morphine. *The most significant change from functional point of view was up-regulation of proteins related to oxidative stress (see discussion for further details).*

Two-dimensional electrophoresis and protein identification in Percoll-purified membranes isolated from brain cortex of control and morphine-treated rats; *analysis by LC-MS/MS*

PM samples were resolved by 2D-electrophoresis in the same way as described for PNS. The resolution in 10% w/v acrylamide/0.26% w/v bis-acrylamide gels was used in the case of silver staining; 12.0% w/v acrylamide/0.32% w/v bis-acrylamide gels were used for staining in CBB. About 300 protein spots were recognized by silver (Figure 2, left panels); when stained in CBB, the total number of detected protein spots was 490 (Figure 2, right panels). Proteins 1–18 with an altered mobility in (+M10) versus (−M10) samples were excised from in

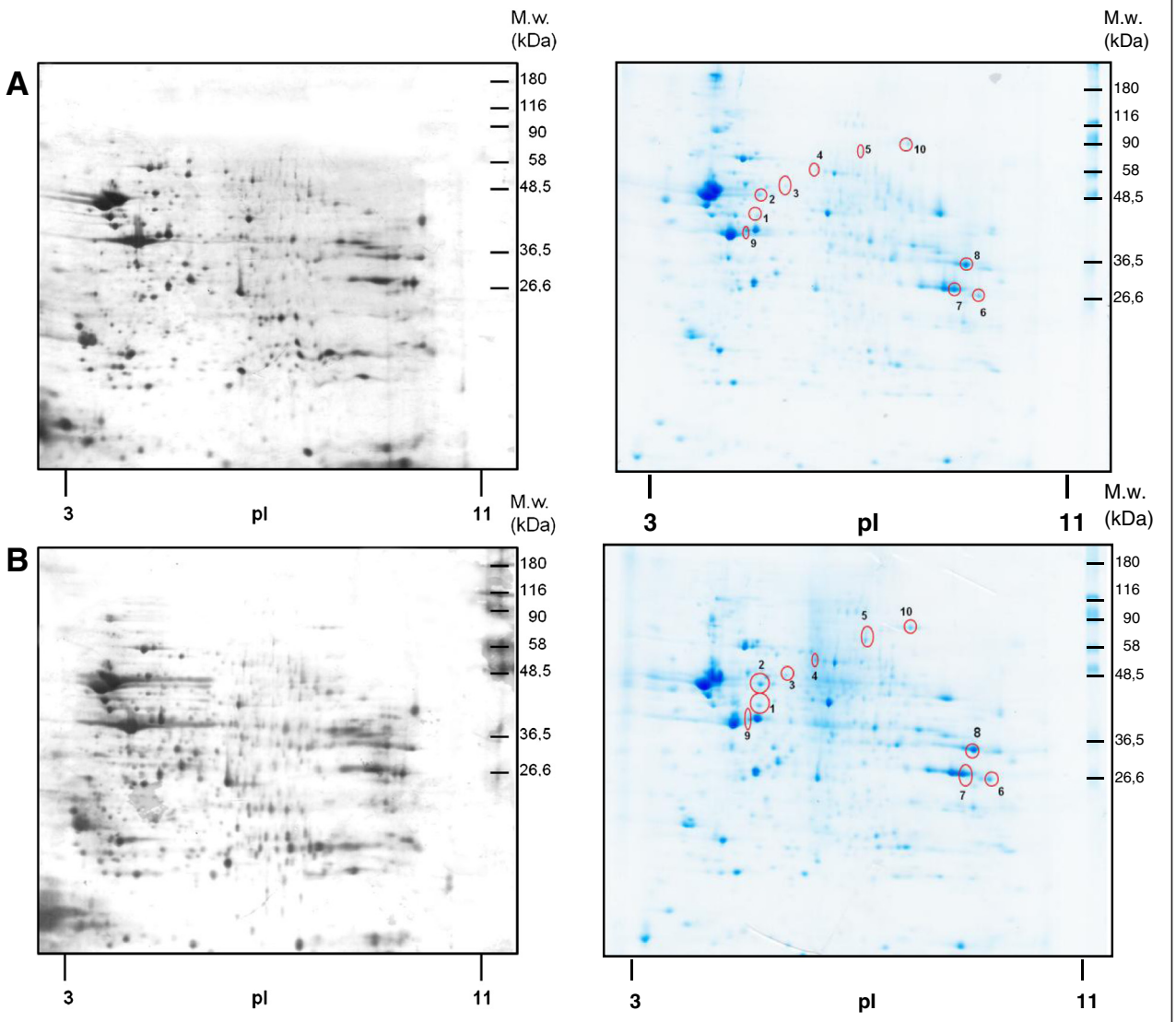

Figure 1 Two-dimensional gel electrophoresis maps of PNS prepared from control (A) and morphine-treated (B) rats. Protein samples (600 μg for both Silver and CBB staining) were separated in the first dimension on pH 3–11 IPG strips. For resolution in the second dimension, SDS-PAGE was performed in 10% w/v acrylamide/0.26% w/v bis-acrylamide gel. The stained 2D gels were scanned in an imaging densitometer and quantified by PDQuest software. The process of quantification of the difference between morphine-treated (+M10) and control (–M10) samples included spot detection, gel matching and spot quantification. Master gel was constructed for each group (+M10) or (–M10) as a synthetic image that contains the spot data from all the gels in the MatchSet. At least four replicates were performed for each group/sample. All matched and unmatched spots were then checked in a manual manner. Protein levels altered at least two-fold were taken into consideration. About 200 protein spots totally were recognized by CBB silver staining by PDQuest analysis. Proteins 1–10 with an altered mobility in (+M10) versus (–M10) samples were excised from in CBB-stained gels and identified by MALDI TOF/TOF analyzer as described in methods. *Left panels*, Silver staining; *Right panels*, CBB staining.

CBB-stained gels and identified by LC-MS/MS. The list of altered and identified proteins is presented in Additional file 2: Table S2 and Table 2. These tables also include a brief description of subcellular localization and function of these proteins as well as quantitative estimate of their relative change induced by morphine-treatment.

The identified up (↑)- or down (↓)-regulated proteins were of *plasma membrane* [**1**-BASP1, Brain acid soluble protein 1, ↓2.1×; **2**-GBB1, Guanine nucleotide-binding protein subunit beta-1, ↓2.0×], *myelin membrane* [**17**-MBP, Myelin basic protein S, ↓2.5×], *cytoplasmic* [**3**-KCRB, Creatine kinase B-type (EC 2.7.3.2), ↓2.6x; **4**-AINX, Alpha-internexin, ↑5.2×; **5**-DPYL2, Dihydropyrimidinase-related protein 2, ↑4.9×; **6**-SIRT2, NAD-dependent deacetylase sirtuin-2, ↑2.5×; **7**-SYUA, Alpha-synuclein, ↑2.0×; **8**-PRDX2, Peroxiredoxin-2, ↑2.2×; **9**-TERA, Transitional endoplasmic reticulum ATPase, ↑2.1×; **13**-UCHL1,

Table 1 Functional significance of proteins identified in PNS as altered by chronic morphine

Protein name	Change (dependence vs.control)	Subcellular localization	Functional category	Protein characterization - PNS
Guanine deaminase	Up-regulated	Cytoplasm	Metabolism	Purine metabolism, guanine degradation [13]
V-type proton ATP subunit B, brain isoform	Up-regulated	Cell membrane	Trafficking	ATP hydrolysis coupled proton transport, vacuolar acidification [14]
Protein disulfide-isomerase A3	Up-regulated	Endoplasmatic reticulum lumen	Cellular development and regulation	Up-regulation of this protein causes apoptotic cell death [15], alterations in its level were revealed during neurodegenerative processes [16]
Dihydropyrimidinase-related protein 2	Up-regulated	Cytoplasm	Neuronal development and regulation	Neuronal development and polarity [8], cone collapse and cell migration; one of major determinants in the control of oxidative stress [17]
N-ethylmaleimide sensitive fusion protein, isoform CRA_a	Up-regulated	Cytoplasm	Trafficking	ATP binding, regulating protein membrane trafficking, involved in vesicle priming [18]
Malate dehydrogenase, mitochondrial precursor	Up-regulated	Mitochondrion matrix	Metabolism	L-malate dehydrogenase activity, protein self-association; up-regulation of the mitochondrial malate dehydrogenase is caused by oxidative stress [19]
Glyceraldehyde-3-phosphate dehydrogenase	Up-regulated	Cytoplasm	Metabolism	Glyceraldehyde-3-phosphate dehydrogenase and nitrosylase activities; surprising role in apoptosis [20]; is known as a major target protein in oxidative stress [21]
Aldolase A	Up-regulated	Mitochondrion	Metabolism	Role in glycolysis and gluconeogenesis, scaffolding protein; potential role in regulating the free intracellular concentration of InsP3, and subsequently intracellular calcium dynamics[22,23]; the expression of aldolase A may be regulated by chronic lithium administration [24]
Creatine kinase B-type	Down-regulated	Cytoplasm	Metabolism	Energy-related (skeletal muscle, heart, brain and spermatozoa), brain development [25]
Aconitate hydratase, mitochondrial precursor	Up-regulated	Mitochondrion	Metabolism	Isomerization of citrate to isocitrate via cis-aconitate;an iron-sulfur protein, the particular susceptibility to oxidative damage may be related to the iron-sulfur cluster [4Fe-4S]in its active site [26]

Ubiquitin carboxyl-terminal hydrolase L1, ↓2.0×; **15**-COR1A, Coronin-1A, ↓5.4×, **16**-SEP11, Septin-11, ↑2.2×; **18**-RL12, 60S ribosomal protein L12, ↑2.7×] and *mitochondrial* [**10**-DHE3, Glutamate dehydrogenase 1, ↑2.7×; **11**-SCOT1, Succinyl-CoA:3-ketoacid-coenzyme A transferase 1, ↑2.2×; **12**-AATM, Aspartate aminotransferase**,** ↓2.2×; **14**-PHB, Prohibitin, ↑2.2×] origin.

Thus, the only member of GPCR-initiated signaling cascades identified by LC-MS/MS was trimeric Gβ subunit, which was decreased 2× in PM samples prepared from morphine-adapted rats. The morphine-induced decrease of Gβ subunit in PM was subsequently verified by immunoblot analysis of the same 2D-gels as those used for preparation of samples for LC-MS/MS (Figure 3). The spot 2 (compare with Figure 2) represented just a small fraction of the total signal of Gβ subunits which was distributed over wider range of pI. The total signal of Gβ was decreased 1.2x only. We have divided the signal of Gβ in CBB-stained gels into 8 small spots according to immunoblot signal (Figure 3) in order to verify it. Proteomic analysis was performed by LC-MS/MS and positive signal was detected in spots 3, 4, 5, 7 and 8 (Table 3).

Therefore, the decrease of Gβ determined by proteomic analysis (2×) has to be regarded as an alternation of relatively small fraction of numerous forms of Gβ resolved by 2D-ELFO. Morphine-induced decrease of Gβ is selectively oriented to specific, minority component of this protein; the dominant pool of Gβ subunits is unchanged.

Discussion

Opium extracts from the plant Papaver somniferum have been used for therapeutic and recreational purposes for thousands of years. Opioid alkaloids and related pharmaceuticals are the most effective analgesics for the treatment of acute and chronic pain. They also represent one of the largest components of the illicit drug market worldwide, generating revenue of approximately $70 billion in 2009, much of which supports crime, wars and terrorism. Intravenous use of opioid drugs is a leading cause of death by overdose in Europe and North America, and a major contributing factor to the worldwide AIDS epidemic [50,51].

Morphine and codeine are the main active opioid alkaloids in opium. In humans, they act on the central nervous system to produce a wide range of effects including analgesia, euphoria, sedation, respiratory depression and cough suppression. Chronic opiate administration results

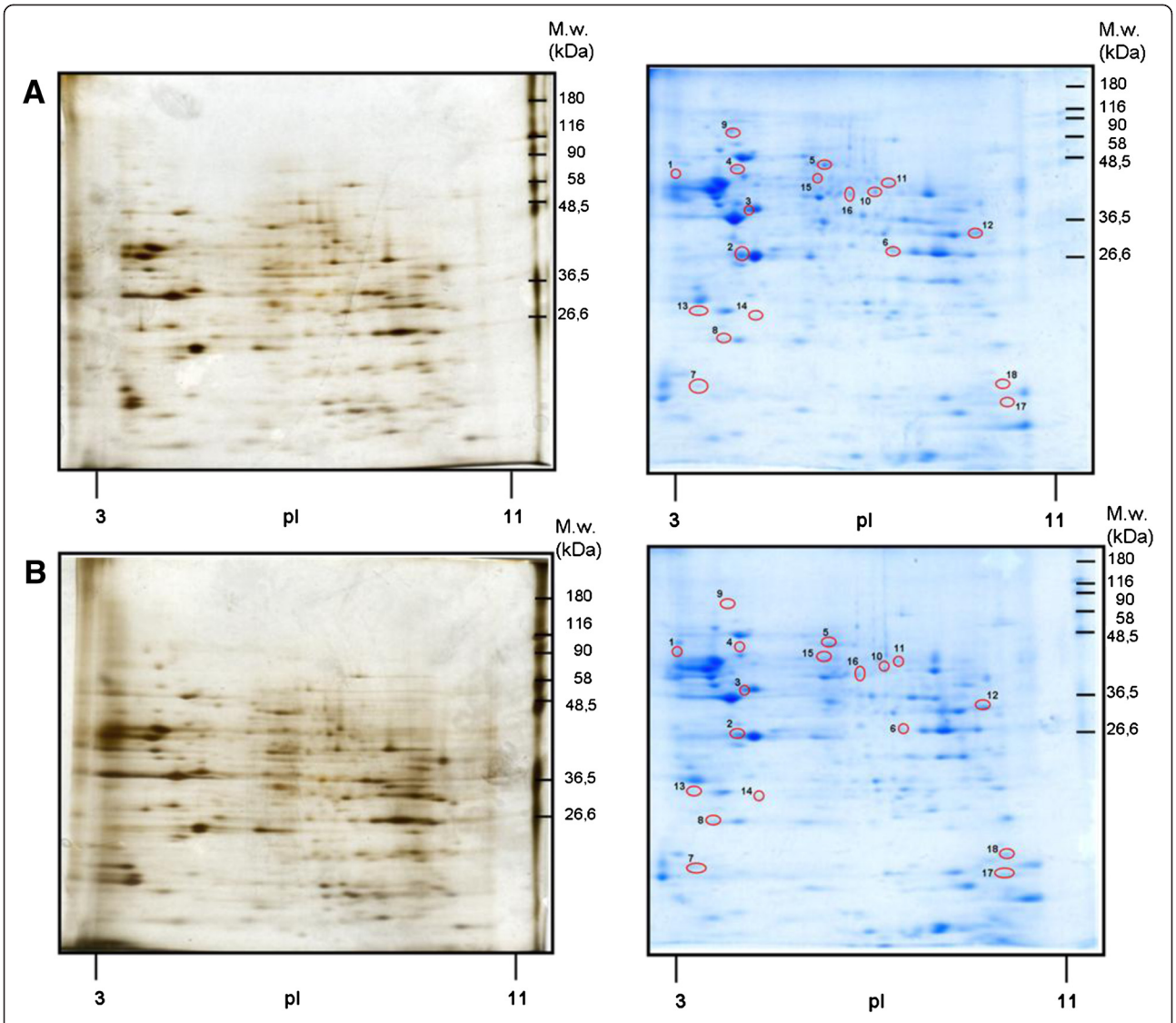

Figure 2 Two-dimensional gel electrophoresis maps of protein extracts prepared from PM of control (A) and morphine-treated (B) rats. Protein samples (400 μg for Silver staining; 2 mg for CBB staining) were separated in the first dimension on pH 3–11 IPG strips. For resolution in the second dimension, SDS-PAGE was performed in 10% w/v acrylamide/0.26% w/v bis-acrylamide gel (silver staining) or in 12.5% w/v acrylamide/0.0625% w/v bis-acrylamide gel (CBB staining). The stained 2D gels were scanned in an imaging densitometer and quantified by PDQuest software. The process of quantification of the difference between morphine-treated (+M10) and control (–M10) samples included spot detection, gel matching and spot quantification. Master gel was constructed for each group (+M10) or (–M10) as a synthetic image that contains the spot data from all the gels in the MatchSet. At least four replicates were performed for each group/sample. All matched and unmatched spots were then checked in a manual manner. Protein levels altered at least two-fold were taken into consideration. About 500 protein spots totally were recognized by CBB staining by PDQuest analysis. Proteins 1–18 with an altered mobility in (+M10) versus (–M10) samples were excised from in CBB-stained gels and identified by LC-MS/MS as described in methods. *Left panels*, Silver staining. *Right panels*, Coomassie staining.

in the development of tolerance and dependence, but the regulation of MOR and DOR function during this process is not clearly understood.

To localize changes of MOR-stimulated G-protein activity in various brain regions after chronic morphine treatment, Sim et al. [52] examined [^{35}S]GTPγS binding to brain sections by in vitro autoradiography. Rats were treated for 12 d with increasing doses (10–320 mg . kg^{-1} . d^{-1}) of morphine. Control rats were injected with either saline or a single acute injection of morphine (20 mg/kg). [^{35}S]GTPγS binding was measured in the presence or absence of MOR-selective agonist DAMGO. In rats injected with a *single acute dose* of morphine, no significant changes were detected in basal or DAMGO-stimulated [^{35}S]GTPγS binding in any brain region. In *chronic morphine-treated rats*, however, DAMGO-stimulated [^{35}S]GTPγS binding in cerebral cortex was significantly decreased when compared with control rats. Similar data were obtained in analysis of

Table 2 Functional significance of proteins identified in PM fraction as altered by chronic morphine

Protein name	Change (dependence vs.control)	Subcellular localization	Functional category	Protein characterization - PM
Brain acid soluble protein 1	Down-regulated	Cell membrane; Lipid anchor	Neuronal development and regulation	Associated with the membranes of growth cones that form the tips of elongating axons, DNA-dependent, localizes in the membrane raft domain with a cholesterol-dependent manner; changes in the localization during the development of neuronal polarity [27]
Guanine nucleotide-binding protein subunit beta-1	Down-regulated	Cell membrane	Signaling	Gβ1 is required for neural tube closure, neural progenitor cell proliferation and neonatal development [28]; stimulated ACII, ACIV, ACVII, inhibited ACI, ACV/VI, ACVIII [29,30]
Creatine kinase B-type	Down-regulated	Cytoplasm	Metabolism	Energy-related (skeletal muscle, heart, brain and spermatozoa), brain development [25], aging [31]; one of major determinants in the control of oxidative stress [17]
Alpha-internexin	Up-regulated	Cytoplasm	Neuronal development and regulation	Copurifies with intermediate filaments from rat spinal cord and optic nerve, developmental protein involved in morphogenesis of neurons [32]
Dihydropyrimidinase-related protein 2	Up-regulated	Cytoplasm	Neuronal development and regulation	Neuronal development and polarity [8], cone collapse and cell migration; one of major determinants in the control of oxidative stress [17]
NAD-dependent deacetylase sirtuin-2	Up-regulated	Cytoplasm	Cellular development and regulation	Colocalizes with microtubules; NAD-dependent deacetylase, involved in the control of mitotic exit in the cell cycle; up-regulation may protect the brain against incurred oxidative damage [33]
Alpha-synuclein	Up-regulated	Cytoplasm	Neuronal development and regulation	Specifically expressed in neuronal cell bodies and synapses, negative regulation of neuron apoptosis, aging; role in the pathogenesis of Parkinson's disease [34]
Peroxiredoxin-2	Up-regulated	Cytoplasm	Neuronal development and regulation	Involved in redox regulation of the cell, negative regulation of neuron apoptosis; the relative abundance appears to protect cellular components by removing the low levels of hydroperoxides and peroxinitrites produced as a result of normal cellular metabolism in the cytosol [35]
Transitional endoplasmic reticulum ATPase	Up-regulated	Cytoplasm Nucleus	Cellular development and regulation	Involved in the formation of the transitional endoplasmatic reticulum, necessary for the fragmentation of Golgi stacks during mitosis and for their reassembly after mitosis [36]; interacts with neurofibromin to control the density of dendritic spines [37]
Glutamate dehydrogenase 1, mitochondrial	Up-regulated	Mitochondrion matrix	Metabolism	Glutamate catabolic process, long-term memory, in rat brain the glutamate dehydrogenase reaction operates in the direction of ammonia production [38]
Succinyl-CoA:3-ketoacid-coenzyme A transferase 1, mitochondrial	Up-regulated	Mitochondrion matrix	Metabolism	A mitochondrial ketone body-activating enzyme [39]; brain development, response to drug
Aspartate aminotransferase, mitochondrial	Down-regulated	Mitochondrion matrix	Metabolism	Amino acid metabolism, metabolite exchange between mitochondria and cytosol, fatty acid transport; its activity is related with the maintenance of amino acid homeostasis and might be an indicator of mitochondrial injury [40]
Ubiquitin carboxyl-terminal hydrolase isozyme L1	Down-regulated	Cytoplasm Endoplasmatic reticulum membrane	Deubiquitination Neuronal development and regulation	Involved both in the processing of ubiquitin precursors and of ubiquitinated proteins; the ubiquitination/proteasome pathway involved in synaptic plasticity [41]
Prohibitin	Up-regulated	Mitochondrion inner membrane	Cellular development and regulation	Antiproliferative activity, role in regulating mitochondrial respiration activity and aging, response to drug [42-44]; down-regulation of prohibitin renders neurons more vulnerable to injury and reactive oxygen species production, whereas up-regulation appears to be neuroprotective [45]
Coronin-1A	Down-regulated	Cytoplasm	Cellular development and regulation	Invagination of plasma membrane, forming protrusions of plasma membrane involved in cell locomotion; coronin-1A activity is spatially and temporally regulated by phosphoinositides [46]

Table 2 Functional significance of proteins identified in PM fraction as altered by chronic morphine *(Continued)*

Septin-11	Up-regulated	Cytoplasm	Cellular development and regulation	Filament-forming cytoskeletal GTPase, cell division; it is involved in dendritic maturation [47]
Myelin basic protein S	Down-regulated	Myelin membrane	Neuronal development and regulation	Myelination, negative regulation of axonogenesis; morphine exposure colud result in a decreased number of myelinated axons [48]
60S ribosomal protein L12	Down-regulated	Cytoplasm	Regulatory	Binds directly to 26S ribosomal RNA; it accesses the importin 11 pathway as a major route into the nucleus [49]

MOR-stimulated [^{35}S]GTPγS binding after chronic heroin administration [53,54]. Accordingly, our analysis of PM isolated from cerebral cortex of rats exposed to morphine for 10 days (10–50 mg/kg) indicated significant desensitization of G-protein response to MOR and DOR stimulation [11] and up-regulation of ACI and II [12].

Proteome changes after prolonged morphine exposure have been so far investigated in "frozen tissue powders" of the rat cerebral cortex, hippocampus, striatum [55,56] and nucleus accumbens [7] or in the "whole-cell lysates" of striatal neuronal cell cultures [57]. Therefore, the aim of our work was to perform proteomic analysis in *more defined* preparations: post-nuclear supernatant (PNS) and membranes isolated in Percoll® gradient (PM). The morphine-induced changes in protein composition (proteom) of PNS and PM were determined by 2D-electrophoresis resolution and PDQuest analysis; the altered proteins were identified by MALDI-TOF MS/MS or LC-MS/MS.

Proteomic analysis of PNS indicated a marked increase of proteins of mitochondrial and cytoplasmic origin (Additional file 1: Table S1 and Table 1). The 9 out of 10 proteins exhibiting the largest morphine-induced change in Coomassie stained gels were increased *by* morphine: **1**-Guanine deaminase, ↑2.5×; **2**-Vacuolar-type proton ATP subunit B, brain isoform ↑2.6×; **3**-Protein disulfide-isomerase A3, ↑3.4×; **4**-Dihydropyrimidinase-related protein 2, ↑3.6x; **5**-N-ethylmaleimide sensitive fusion protein, isoform CRAa, ↑2.0×; **6**-Malate dehydrogenase, mitochondrial precursor, ↑1.4×; **7**-Glyceraldehyde-3-phosphate dehydrogenase, ↑1.6×; **8**-Aldolase A, ↑1.3×; **10**-Aconitate hydratase, mitochondrial precursor, ↑1.3×**.** The 4 out of 9 up-regulated proteins (**4**, **6**, **7**, **10**) were described as functionally related to manifestation of oxidative stress conditions [17,19,21,26]. Marked increase of Protein disulfide-isomerase A3 (**3**) causing apoptotic cell death [15] should be also noticed. The role in apoptosis has

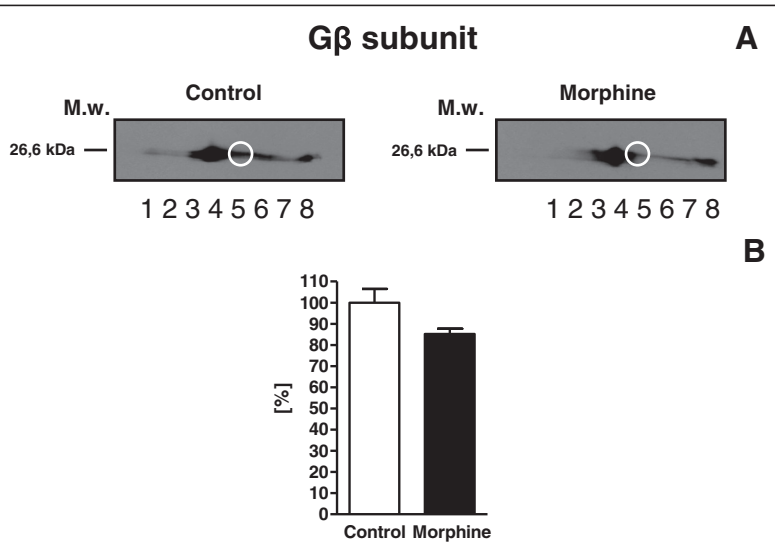

Figure 3 Gβ subunit protein; ***immunoblot analysis of 2D-gels.*** **A** Two-dimensional resolution of Gβ protein content in PM isolated from control and morphine-adapted rats. PM protein (400 μg) was resolved by 2D electrophoresis using the pI range 3–11 for isoelectric focusing in the first dimension. The white small circle shows the small fraction of the the total signal of Gβ which was taken into consideration when analyzed by LC-MS/MS. The second dimension was performed by SDS-PAGE in 10% w/v acrylamide/0.26% bis-acrylamide gels (Hoefer SE 600). Gβ was identified by immunoblotting with specific antibody as described in Material and methods. The numbers 1–8 represent spots of Gβ subunits which were subsequently analyzed by LC-MS/MS. **B** The average of 3 immunoblots ± SEM. Difference between (–M10) and (+M10) was analyzed by Student's *t*-test using GraphPad*Prizm4* and found not significant, NS ($p > 0.05$).

Table 3 Proteomic analysis of Gβ subunits isolated from brain cortex of control and morphine-treated rats

Spot	Accession number	Protein name	Mascot score	Matched peptides	Peptides	SC[a] [%]	MW[b] (kDa)	pI[c]
3	GBB1_RAT	**Guanine nucleotide-binding protein subunit beta-1**	184.3	6	R.LFDLR.A R.LLVSASQDGK.L K.LWDVR.E K.IYAMHWGTDSR.L + Oxidation (M) K.ACADATLSQITNNIDPVGR.I K.VHAIPLR.S	16.8	37.4	5.6
4	GBB1_RAT	**Guanine nucleotide-binding protein subunit beta-1**	471	12	K.ACADATLSQITNNIDPVGR.I R.LFVSGACDASAK.L K.IYAMHWGTDSR.L + Oxidation (M) R.LFDLR.A K.IYAMHWGTDSR.L R.LLVSASQDGK.L K.LWDVR.E R.KACADATLSQITNNIDPVGR.I R.LLLAGYDDFNCNVWDALK.A K.VHAIPLR.S K.LIIWDSYTTNK.V R.ELAGHTGYLSCCR.F	32.9	37.4	5.6
4	GBB2_RAT	**Guanine nucleotide-binding protein subunit beta-2**	413.9	10	R.TFVSGACDASIK.L K.ACGDSTLTQITAGLDPVGR.I K.IYAMHWGTDSR.L + Oxidation (M) R.LFDLR.A K.IYAMHWGTDSR.L R.LLVSASQDGK.L K.LWDVR.D K.VHAIPLR.S K.LIIWDSYTTNK.V R.LLLAGYDDFNCNIWDAMK.G + Oxidation (W)	14.4	37.3	5.6
5	GBB1_RAT	**Guanine nucleotide-binding protein subunit beta-1**	199.1	5	R.AGVLAGHDNR.V R.LFVSGACDASAK.L R.LFDLR.A K.IYAMHWGTDSR.L + Oxidation (M) R.LLVSASQDGK.L	14.1	37.4	5.6
5	GBB2_RAT	**Guanine nucleotide-binding protein subunit beta-2**	188.7	5	R.AGVLAGHDNR.V R.TFVSGACDASIK.L R.LFDLR.A K.IYAMHWGTDSR.L + Oxidation (M) R.LLVSASQDGK.L	3.5	37.3	5.6
7	GBB (1–4)_RAT	**Guanine nucleotide-binding protein subunit beta-3**	22.4	1	K.LLVSASQDGK.L	2.9	37.2	5.4
8	GBB (1–4)_RAT	**Guanine nucleotide-binding protein subunit beta-3**	34.7	1	K.LLVSASQDGK.L	2.9	37.2	5.4

[a]Sequence coverage.
[b]Theoretical molecular weight.
[c]Theoretical isoelectric point.

been also described for Glyceraldehyde-3-phosphate dehydrogenase (**7**), already mentioned as major target protein in oxidative stress [21]. The 4 out of 9 up-regulated proteins (**4**, **6**, **7**, **10**) were thus functionally related to manifestation of the state of oxidative stress/oxidative damage in brain of morphine-exposed rats and 2 proteins were related to apoptotic cell death.

More detailed analysis of Percoll-purified membranes indicated a complex reorganization of PM protein composition. The list of proteins presented in Additional file 2: Table S2 and Table 2 indicates that morphine-induced alternation included increase as well as decrease of wide range of proteins functionally and structurally related to plasma, myelin, endoplasmic reticulum and mitochondrial membranes. Numerous soluble enzymes present in soluble, cytosol fraction or in mitochondrial matrix were also altered by chronic morphine. Surprisingly, with the exception of trimeric Gβ subunit, not just one of these proteins was functionally related to GPCR- or ionic-channel-activated signaling cascades. Similarly, proteomic analysis of protein alternations induced in the long-term TRH-treatment of HEK cells expressing TRH-R and G11α protein indicated the change of 42 proteins, but not even one of these proteins represented plasma membrane protein functionally related to GPCR-initiated signaling cascades [58].

Our results indicate that the energy metabolism of rat brain cortex exposed to increasing doses of morphine (10–50 mg/kg, 10 days) is shifted far from the normal, physiological state. Using other words, brain cortex of rats exposed to morphine according to our protocol is far from being adapted. It may be suggested that the both neuronal and glial cells undergo a drastic reorganization as consequence of cell discomfort and, subsequently, oxidative stress. Simultaneous activation of all types of opioid receptors (μ-, δ- and κ-OR) by high doses of morphine results in high energy demand of neurons [59,60]. Consequently, glycogen in astrocytes as the single largest energy reserve in the brain is mobilized with the aim to match these increased energy requirements [61]. After depletion of glycogen in astrocytes, the state of oxidative stress appears [62] as the full supply of oxygen to brain mitochondria is not accompanied by transfer of the sufficient number of "reducing equivalents" into the mitochondrial matrix.

Conclusions

Proteomic analysis of rat brain cortex of rats exposed to morphine for 10 days (10–50 mg/kg) indicated a significant morphine-induced change of membrane protein composition. Changes in *post-nuclear supernatant* were exclusively based on increase (1.3-3.6×) of proteins of mitochondrial and cytoplasmic origin. In isolated *plasma membranes* (PM), morphine-induced alternation included increase as well as decrease of wide range of proteins functionally and structurally related to plasma, myelin, endoplasmic reticulum and mitochondrial membranes. Numerous soluble enzymes present in soluble, cytosol fraction or in mitochondrial matrix were also altered by chronic morphine. The only member of GPCR-initiated signaling cascades identified by LC-MS/MS in Percoll-purified membranes was trimeric Gβ subunit (**2**-GBB) which was decreased 2x in samples prepared from morphine-adapted rats. This "active" component of Gβ subunits, however, represented a minor pool of total complement of Gβ molecules in PM, which was unchanged.

Material and methods

Chemicals

Acrylamide, bis-acrylamide and Coomassie Blue G-250 were from SERVA (Heidelberg, Germany), nitrocellulose membrane was from Whatman (Germany). Immobiline Dry-Strips, Pharmalyte buffer, and secondary anti-rabbit antibody labeled with horseradish peroxidase were purchased from GE Healthcare (Piscataway, NJ). Complete protease inhibitor cocktail was from Roche Diagnostic, Mannheim, Germany (cat. no. 1697498). All others chemicals were from Sigma-Aldrich and were of highest purity available. Primary antibody oriented against trimeric Gβ subunit protein (T-20, sc-378) was from Santa Cruz.

Animals

Male Wistar rats (220-250 g) were killed by decapitation under ether narcosis, the frontal brain was rapidly removed, washed intensively from the remaining blood and cooled to 0°C. The cerebral cortex was separated on the pre-cooled plate, snap frozen in liquid nitrogen and stored at −70°C until use. The experiments were approved by Animal Care and Use Committee of the Institute of Physiology, Academy of Sciences of the Czech Republic to be in agreement with Animal Protection Law of the Czech Republic as well as European Comunity Council directives 86/609/EEC.

Morphine treatment of experimental animals

The animals were exposed to morphine by intra-muscular application according to the following protocol: 10 mg/kg (day 1 and 2), 15 mg/kg (day 3 and 4), 20 mg/kg (day 4 and 5), 30 mg/kg (day 6 and 7), 40 mg/kg (day 9) and, finally 50 mg/kg (day 10). The *morphine-adapted* rats were sacrificed 24 hours after the last dose of the drug (group + M10). Control animals were injected with sterile PBS and sacrificed in parallel with morphine-treated rats, i.e. 24 hours (group – M10) after the last dose [12].

Subcellular fractionation of rat brain cerebral cortex; preparation of post-nuclear supernatant (PNS) and percoll-purified membranes (PM)

Rat brain cortex was minced with razor blade on pre-cooled plate and diluted in STEM medium containing 250 mM sucrose, 20 mM Tris–HCl, 3 mM $MgCl_2$, 1 mM EDTA, pH 7.6, fresh 1 mM PMSF plus protease inhibitor cocktail. It was then homogenized mildly in loosely-fitting Teflon-glass homogenizer for 5 min (2 g w. w. per 10 ml) and centrifuged for 5 min at 3500 rpm (1200 × *g*). Resulting post-nuclear supernatant (PNS) was filtered through Nylon nets of decreasing size (330, 110 and 75 mesh, Nitex) and applied on top of Percoll in Beckman Ti70 tubes (30 ml of 27.4% Percoll in STE medium). Centrifugation for 60 min at 30000 rpm (65000 × *g*) resulted in the separation of two clearly visible layers (Bourova et al., 2009). The upper layer represented plasma membrane fraction (PM); the lower layer contained mitochondria (MITO). The upper layer was removed, diluted 1:3 in STEM medium and centrifuged in Beckman Ti70 rotor for 90 min at 50000 rpm (175000 × *g*). Membrane sediment was removed from the compact, gel-like sediment of Percoll and re-homogenized by hand in a small volume of 50 mM Tris–HCl, 3 mM $MgCl_2$, 1 mM EDTA, pH 7.4 (TME medium).

SDS-PAGE and immunoblotting

The aliquots of membrane fractions were mixed 1:1 with 2x concentrated Laemmli buffer (SLB) and heated for 3 min at 95 °C. Standard (10% w/v acrylamide/0.26% w/v bis-acrylamide) SDS electrophoresis was carried out as described before [63-65]. Molecular mass determinations were based on pre-stained molecular mass markers (Sigma, SDS 7B). After SDS-PAGE, proteins were transferred to nitrocellulose and blocked for 1 h at room temperature in 5% (w/v) low-fat milk in TBS-Tween buffer [10 mM Tris–HCl, pH 8.0, 150 mM NaCl, 0.1% (v/v) Tween 20]. Antibodies were added in TBS-Tween containing 1% (w/v) low-fat milk and incubated for at least 2 h. The primary antibody was then removed and the blot washed extensively (3x10 min) in TBS-Tween. Secondary antibodies (donkey anti-rabbit IgG conjugated with horseradish peroxidase) were diluted in TBS-Tween containing 1% (w/v) low-fat milk, applied for 1 h and after three 10 min washes, the blots were developed by ECL technique using Super Signal West Dura (Pierce) as substrate. The developed blots were scanned with an imaging densitometer ScanJett 5370C (HP) and quantified by Aida Image Analyzer v. 3.28 (Ray test).

Sample preparation for isoelectric focusing

Samples of PNS or PM containing 400–600 μg protein or 2 mg protein, respectively, were precipitated with ice cold aceton overnight at – 20°C. After centrifugation at 16 000 × *g* for 20 min at 4°C, the supernatant was removed and the pellet was precipitated with ice-cold 6% TCA for 1.5 h on ice. After centrifugation at 16 000 × *g* for 10 min at 4°C, the supernatant was discarded and the pellet washed with 400 μl of ice-cold 96% ethanol for 1 h at room temperature. The mixture was centrifuged at 16 000 × *g* for 10 min at 4°C and the remaining pellet was solubilizated with 250 μl IEF sample buffer containing 7 M urea, 2 M thiourea, 4% CHAPS, 1% DTT, 1% ampholines pH 3–10 and 0.01% bromphenol blue for 3 h at room temperature. After a brief centrifugation (16 000 × *g*, 1 min), the sample was transferred into a groove of the Immobiline DryStrip Reswelling Tray (GE Healthcare).

Two-dimensional electrophoresis (2D-ELFO)

Immobiline DryStrips (linear pH gradient 3–11 NL, 13 cm) were placed into the Immobiline DryStrip Reswelling Tray containing protein samples and rehydrated overnight.

Isoelectric focusing was performed using the Multiphor II system (GE Healthcare) at 15°C in the following manner: 150 V for 5 h, 500 V for 1 h, 3500 V for 12 h and 500 V for 3 h. The focused strips were stored at – 20°C or immediately used.

Strips were rinsed thoroughly with ultrapure water, dried quickly on filter paper and equilibrated in 4 ml of equilibration buffer (50 mM Tris–HCl pH 6.8, 6 M urea, 0.1 mM EDTA, 2% SDS, 30% glycerol and 0.01% bromophenol blue) containing 1% DTT for 15 min in order to reduce disulphide bridges and other oxidized groups. Subsequently, the strips were alkylated in equilibration buffer containing 2.5% iodoacetamide for 15 min. Molecular weight markers were loaded onto a piece of filter paper and placed close to the alkaline side of the strip. The strip and molecular marker were covered with 0.5% agarose. Gels were run vertically at a constant current of 10 mA for 20 min and then at 80 mA for 2 h till the bromophenol blue dye reached the end of the gel. The apparatus was cooled to 15°C using the Hoefer SE 600 unit (GE Healthcare).

Silver staining

Silver staining was performed by ProteoSilver™ Plus Silver Stain Kit (Sigma-Aldrich) according to the manufacturer's instructions [66-68]. Briefly, the gel was fixed in 40% ethanol/10% acidic acid overnight and then washed by 30% ethanol for 10 min and once by ultrapure water for 10 min. The gels were incubated for 10 min with 1% Sensitizer solution and washed twice with 200 ml of ultrapure water for 10 min. The gels were submerged in 1% Silver solution for 10 min, washed with 200 ml of ultrapure water for 1 min and developed with 100 ml of the Developer solution until the desired

intensity of spots was attained. The ProteoSilver Stop solution was added to the Developer solution and gels were incubated for 5 min. All steps were carried out at room temperature on an orbital shaker at 60 to 70 rpm. The gels were stored in fresh, ultrapure water or dried in 3% glycerol/25% methanol.

Colloidal coomassie staining

For MS analysis, the gels were stained by colloidal Coomassie Blue G-250 [69]. The gel was fixed in 40% methanol/5% orthophosphoric acid for 12 h and incubated with colloidal Coomassie Blue (17% ammonium sulphate, 34% methanol, 3% orthophosphoric acid and 0.1% Coomassie G-250) for 48 h. After staining, the gels were kept in 1% acetic acid at 4°C.

Image analysis

The stained 2D gels were scanned with an imaging densitometer ScanJett 5370C (HP) and quantified by PDQuest software (Bio-Rad, version 7.3.1). The process included spot detection, gel matching and spot quantification. Master gel was constructed as a synthetic image that contains the spot data from all the gels in the MatchSet. At least four replicates were performed for each sample. All matched and unmatched spots were then checked in a manual manner. Protein levels altered at least two-fold were taken into consideration.

Preparation of samples for MALDI-TOF MS/MS; *analysis of post-nuclear fraction*

Mass spectrometric analysis MALDI-TOF was performed as described before [58]. The peak lists from the MS spectra were generated by 4000 Series Explorer V 3.5.3 (Applied Biosystems/MDS Sciex) without smoothing, peaks with local signal to noise ratio greater than 5 were picked and searched by local Mascot v. 2.1 (Matrix Science) against nonredundant NCBI database of protein sequences (11186807 sequences; 3815639892 residues). Database search criteria were as follows-enzyme: trypsin, taxonomy: *Rattus norvegicus* (66703 sequences), fixed modification: carbamidomethylation, variable modification: methionine oxidation, peptide mass tolerance: 120 ppm, one missed cleavage allowed. Only hits that were scored as significant ($P < 0.001$) were included.

In-gel digestion and preparation of samples for LC-MS/MS; *analysis of percoll-purified membranes (PM)*

Protein spots (from 2-DE: ca 1–2 mm in diameter) were excised from the Coomassie-stained gels, and then processed as described by Shevchenko et al. [70]. Briefly, the spots were first destained by incubation in 100 μl of 100 mM ammonium bicarbonate/acetonitrile (1:1, v/v) with occasional shaking for 1 hour. After destaining, the gel pieces were shrunk by dehydration in 500 μl of acetonitrile, which was then removed and the gel pieces were dried in a vacuum centrifuge. In further step, 100 μl of 10 mM DTT in 100 mM ammonium bicarbonate was added, and the proteins were reduced for 1 hour at 56°C. After cooling to room temperature, the DTT solution was replaced by roughly the same volume of 55 mM iodoacetamide in 100 mM ammonium bicarbonate, and the gels were incubated at ambient temperature for 45 min in the dark. Then the gel pieces were washed with 100 μl of 100 mM ammonium bicarbonate, and dehydrated by addition 500 μl of acetonitrile. Subsequently, the liquid phase was removed and the gel pieces were dried in a vacuum centrifuge.

Before the in-gel digestion, the gel pieces were cooled in an ice-cold bath and swollen in a 100 μl of digestion buffer containing trypsin (20 μg/ml) in 50 mM ammonium bicarbonate, and the gel pieces were sonicated (5 min), placed to air circulation thermostat, and incubated overnight at 37°C. The volumes of solutions needed for processing of the protein bands were four-fold larger than the volumes for processing of the spots. The supernatant of each spot was then transferred to a new vial. The in-gel digestion was performed once more the same way. The resulting tryptic peptides were extracted with sonication (15 min) by 150 μl of extraction buffer (5% formic acid/acetonitrile, 1:2, v/v). Then the solution was spun, the supernatants were transferred, pooled and concentrated to dryness by lyophilization. Dried extracts were stored at −80°C before analysis.

Analysis of tryptic digests with LC-MS/MS

Dried protein digests were dissolved in 20 μl of 1% formic acid, centrifuged (10 000 × *g*, 5 min, 4°C) and the supernatant transferred to inserts in vials. The nano-HPLC apparatus used for protein digests analysis was a Proxeon Easy-nLC (Proxeon, Odense, Denmark) coupled to a maXis Q-TOF (quadrupole – time of flight) mass spectrometer with ultrahigh resolution (Bruker Daltonics, Bremen, Germany) by nanoelectrosprayer. The nLC-MS/MS instruments were controlled with the software packages HyStar 3.2 and micrOTOF-control 3.0. The data were collected and manipulated with the software packages ProteinScape 2.0 and DataAnalysis 4.0 (Bruker Daltonics).

The 3 μl of the peptide mixture were injected into a NS-AC-11-C18 Biosphere C18 column (particle size: 5 μm, pore size: 12 nm, length: 150 mm, inner diameter: 75 μm), with a NS-MP-10 Biosphere C18 pre-column (particle size: 5 μm, pore size: 12 nm, length: 20 mm, inner diameter: 100 μm), both manufactured by NanoSeparations (Nieuwkoop, Netherlands).

The separation of peptides was achieved via a linear gradient between mobile phase A (water) and B (acetonitrile), both containing 0.1% (v/v) formic acid. Separation was

started by running the system with 5% mobile phase B, followed by gradient elution to 30% B at 70 min. The next step was gradient elution to 50% B in 10 min, and then a gradient to 100% B in 8 min was used. Finally, the column was eluted with 100% B for 2 min. Equlibration before the next run was achieved by washing the column with 5% mobile phase B for 10 min. The flow rate was 0.25 μl min^{-1}, and the column was held at ambient temperature (25°C).

On-line nano-electrospray ionization (easy nano-ESI) in positive mode was used. The ESI voltage was set at +4.5 kV, scan time 1.3 Hz. Operating conditions: drying gas (N_2), 1 l min^{-1}; drying gas temperature, 160°C; nebulizer pressure, 0.4 bar. Experiments were performed by scanning from 100 to 2200 m/z. The reference ion used (internal mass lock) was a monocharged ion of $C_{24}H_{19}F_{36}N_3O_6P_3$ (m/z 1221.9906). Mass spectra corresponding to each signal from the total ion current chromatogram were averaged, enabling an accurate molecular mass determination. All LC-MS/MS analyses were done in duplicates.

Database searching

Data were processed using ProteinScape software. Proteins were identified by correlating tandem mass spectra to SwissProt databases, using the MASCOT searching engine (http://www.matrixscience.com); *Rattus norvegicus* as species. Trypsin was chosen as the enzyme parameter. One missed cleavage was allowed, and an initial peptide mass tolerance of ±10.0 ppm was used for MS and ±0.05 Da for MS/MS analysis. Cysteines were assumed to be carbamidomethylated, proline and lysine to be hydroxylated, serine, threonine and tyrosine to be phosphorylated, and methionine was allowed to be oxidated. All these possible modifications were set to be variable. Monoisotopic peptide charge was set to 1+, 2+ and 3+. The Peptide Decoy option was selected during the data search process to remove false-positive results. Only significant hits (MASCOT score ≥60, http://www.matrixscience.com) were accepted.

Statistical analysis

In immunoblot assays, the significance of difference between data collected in control and morphine-treated samples was analyzed by Student's t-test by GraphPad-*Prizm4*. Results represent the average ± S.E.M.

Protein determination

The method of Lowry was used for determination of membrane protein. Bovine serum albumin (Sigma, Fraction V) was used as standard. Data were calculated by fitting the data with calibration curve as quadratic equation.

Additional files

Additional file 1: Table S1. Proteomic analysis of post-nuclear supernatant prepared from brain cortex of control and morphine-treated rats.

Additional file 2: Table S2. Proteomic analysis of PM fraction isolated from brain cortex of control and morphine-treated rats.

Abbreviations

AC: Adenylyl cyclase; CBB: Coomassie brilliant blue; d: Day; DAMGO: [(2-D-alanine2-4-methylphenylalanine-5-glycineol)-enkefalin]; DADLE: [(2-D-alanine-5-D-leucine)-enkefalin]; DOR: δ-opioid receptor; DTT: Dithiothreitol; EDTA: Ethylenediamine-tetraacetic acid; ELFO: Electrophoresis; GPCR: G protein-coupled receptor; G proteins: Heterotrimeric guanine nucleotide-binding regulatory proteins; CHAPS: 3-[(3-cholamidopropyl) dimethylammonio]-1-propanesulfonate; DTT: Dithiothreitol; IEF: Isoelectric focusing; KOR: κ-opioid receptor; LC-MS/MS: Liquid chromatography–mass spectrometry; MALDI-TOF MS/MS: Matrix-assisted laser desorption/ionization time-of-flight mass spectrometry; MOR: μ-opioid receptor; PBS: Phosphate-buffered saline; PM: Percoll®-purified membranes; PMSF: Phenylmethylsulfonyl fluoride; PNS: Post-nuclear supernatant; SLB: Sample loading buffer; TBS: Tris-buffered saline; w.w.: Wet weight; TCA: Trichloroacetic acid; TRH-R: Thyrotropin-releasing hormone receptor.

Competing interests

The authors declare that they have no competing interests.

Authors' contributions

HU performed the experiments, analyzed the data and participated in writing the manuscript. AE performed proteomic analysis of plasma membrane proteins by LC-MS/MS. DK and LB were responsible for application of morphine to rats according to experimental protocol described in Methods and prepared membrane fractions by differential or density gradient centrifugation. PS conceived the study, designed the experiments and wrote the manuscript. All authors have read and approved the final manuscript.

Acknowledgements

This work was supported by the GACR (P207/12/0919), Centrum of Neurosciences (P304/12/G069) and by Academy of Sciences of the Czech Republic (RVO: 67985823). The authors thank to Silvia Bezouskova for useful practical experience, Petr Jedelsky for performing MALDI -TOF MS/MS and Karel Harant for valuable assistance.

Author details

[1]Laboratories of Biochemistry of Membrane Receptors, Institute of Physiology, v.v.i., Academy of Sciences of the Czech Republic, Videnska 1083, Prague 4 14220, Czech Republic. [2]Analysis of Biologically Important Compounds, Institute of Physiology, v.v.i., Academy of Sciences of the Czech Republic, Videnska 1083, Prague 4 14220, Czech Republic.

Received: 2 July 2013 Accepted: 3 February 2014
Published: 14 February 2014

References

1. Contet C, Kieffer BL, Befort K: **Mu opioid receptor: a gateway to drug addiction.** *Curr Opin Neurobiol* 2004, **14:**370–378.
2. Preston KL: **Drug abstinence effects: opioids.** *Br J Addict* 1991, **86:**1641–1646.
3. Connor M, Christie MD: **Opioid receptor signalling mechanisms.** *Clin Exp Pharmacol Physiol* 1999, **26:**493–499.
4. Law PY, Wong YH, Loh HH: **Molecular mechanisms and regulation of opioid receptor signaling.** *Annu Rev Pharmacol Toxicol* 2000, **40:**389–430.
5. Law PY, Loh HH, Wei LN: **Insights into the receptor transcription and signaling: implications in opioid tolerance and dependence.** *Neuropharmacology* 2004, **47:**300–311.
6. Robinson TE, Kolb B: **Morphine alters the structure of neurons in the nucleus accumbens and neocortex of rats.** *Synapse* 1999, **33:**160–162.

7. Li KW, Jimenez CR, van der Schors RC, Hornshaw MP, Schoffelmeer ANM, Smit AB: **Intermittent administration of morphine alters protein expression in rat nucleus accumbens.** *Proteomics* 2006, **6:**2003–2008.
8. Kim SY, Chudapongse N, Lee SM, Levin MC, Oh JT, Park HJ, Ho IK: **Proteomic analysis of phosphotyrosyl proteins in morphine-dependent rat brains.** *Brain Res Mol Brain Res* 2005, **133:**58–70.
9. Miller AL, Hawkins RA, Harris RL, Veech RL: **The effects of acute and chronic morphine treatment and of morphine withdrawal on rat brain in vivo.** *Biochem J* 1972, **129:**463–469.
10. Li Q, Zhao X, Zhong LJ, Yang HY, Wang Q, Pu XP: **Effects of chronic morphine treatment on protein expression in rat dorsal root ganglia.** *Eur J Pharmacol* 2009, **612:**21–28.
11. Bourova L, Vosahlikova M, Kagan D, Dlouha K, Novotny J, Svoboda P: **Long-term adaptation to high doses of morphine causes desensitization of μ-OR- and δ-OR-stimulated G-protein response in forebrain cortex but does not decrease the amount of G-protein alpha subunit.** *Med Sci Monit* 2010, **16:**260–270.
12. Ujcikova H, Dlouha K, Roubalova L, Vosahlikova M, Kagan D, Svoboda P: **Up-regulation of adenylylcyclases I and II induced by long-term adaptation of rats to morphine fades away 20 days after morphine withdrawal.** *Biochim Biophys Acta* 1810, **2011:**1220–1229.
13. Paletzki RF: **Cloning and characterization of guanine deaminase from mouse and rat brain.** *Neuroscience* 2002, **109:**15–26.
14. Toei M, Saum R, Forgac M: **Regulation and isoform function of the V-ATPases.** *Biochemistry* 2010, **49:**4715–4723.
15. Tanaka S, Uehara T, Nomura Y: **Up-regulation of protein-disulfide isomerase in response to hypoxia/brain ischemia and its protective effect against apoptotic cell death.** *J Bioch Chem* 2000, **275:**10388–10393.
16. Conn KJ, Gao W, McKee A, Lan MS, Ullman MD, Eisenhauer PB, Fine RE, Wells JM: **Identification of the protein disulfide isomerase family member PDIp in experimental Parkinson's disease and Lewy body pathology.** *Brain Res* 2004, **1022:**164–172.
17. Drabik A, Bierczynska-Krzysik A, Bodzon-Kulakowska A, Suder P, Kotlinska J, Silberring J: **Proteomics in neurosciences.** *Mass Spectrom Rev* 2007, **26:**432–450.
18. Abul-Husn NS, Annangudi SP, Ma'ayan A, Ramos-Ortolaza DL, Stockton SD Jr, Gomes I, Sweedler JV, Devi LA: **Chronic morphine alter the presynaptic protein profile: identification of novel molecular targets using proteomics and network analysis.** *PLoS One* 2011, **6:**e25535.
19. Shi Q, Gibson GE: **Up-regulation of the mitochondrial malate dehydrogenase by oxidative stress in mediated by miR-743a.** *J Neurochem* 2011, **118:**440–448.
20. Chuang DM, Hough C, Senatorov VV: **Glyceraldehyde-3-phosphate dehydrogenase, apoptosis, and neurodegenerative diseases.** *Annu Rev Pharmacol Toxicol* 2005, **45:**269–290.
21. Hwang NR, Yim SH, Kim YM, Jeong J, Song EJ, Lee Y, Choi S, Lee KJ: **Oxidative modifications of glyceraldehyde-3-phophate dehydrogenase play a key role in its multiple cellular functions.** *Biochem J* 2009, **423:**253–264.
22. Koppitz B, Vogel F, Mayr GW: **Mammalian aldolases are isomer-selective high-affinity inositol polyphosphate binders.** *Eur J Biochem* 1986, **161:**421–433.
23. Baron CB, Tolan DR, Choi KH, Coburn RF: **Aldolase A Ins(1,4,5)P_3-binding domains as determined by site-directed mutagenesis.** *Biochem J* 1999, **341:**805–812.
24. Hua LV, Green M, Warsh JJ, Li PP: **Lithium regulation of aldolase A expression in the rat frontal cortex: identification by differential display.** *Biol Psychiatry* 2000, **48:**58–64.
25. Shen W, Willis D, Zhang Y, Schlattner U, Wallimann T, Molloy GR: **Expression of creatine kinase isoenzyme genes during postnatal development of rat brain cerebellum:evidence for transcriptional regulation.** *Biochem J* 2002, **367:**369–380.
26. Perluigi M, Poon HF, Maragos W, Pierce WM, Klein JB, Calabrese V, Cini C, De Marco C, Butterfield DA: **Proteomic analysis of protein expression and oxidative modification in R6/2 transgenic mice.** *Mol Cell Proteomics* 2005, **4:**1849–1861.
27. Kashihara M, Miyata S, Kumanogoh H, Funatsu N, Matsunaga W, Kiyohara T, Sokawa Y, Maekawa S: **Changes in the localization of NAP-22, a calmodulin binding membrane protein, during the development of neuronal polarity.** *Neurosci Res* 2000, **37:**315–325.
28. Okae H, Iwakura Y: **Neural tube defects and impaired neural progenitor cell proliferation in Gβ_1-deficient mice.** *Dev Dyn* 2010, **239:**1089–1101.
29. Sunahara RK, Taussig R: **Isoforms of mammalian adenylylcyclase: multiplicities of signaling.** *Mol Interv* 2002, **2:**168–184.
30. Wang HY, Burns LH: **Gβγ that interacts with adenylyl cyclase in opioid tolerance originates from a Gs protein.** *J Neurobiol* 2006, **12:**1302–1310.
31. Perluigi M, Domenico FD, Giorgi A, Shininà ME, Coccia R, Cini C, Bellia F, Cambria MT, Cornelius C, Butterfield DA, Calabrese V: **Redox proteomics in aging rat brain involvement of mitochondrial reduced glutathione status and mitochondrial protein oxidation in the aging process.** *J Neurosci Res* 2010, **88:**3498–3507.
32. Kaplan MP, Chin SSM, Fliegner KH, Liem RKH: **α-internexin, a novel neuronal intermediate filament protein, precedes the low molecular weight neurofilament protein (NF-L) in the developing rat brain.** *J Neurosci* 1990, **10:**2735–2748.
33. Wu A, Ying Z, Gomez-Pinilla F: **Oxidative stress modulates Sir2α in rat hippocampus and cerebral cortex.** *Eur J Neurosci* 2006, **22:**5213–5216.
34. Maries E, Dass B, Collier TJ, Kordower JH, Steece-Collier K: **The role of α-synuclein in Parkinson's disease: insights from animal models.** *Nat Rev Neurosci* 2003, **4:**727–738.
35. Rhee SG, Chae HZ, Kim K: **Peroxiredoxins: a historical overview and speculative preview of novel mechanisms and emerging concepts in cell signaling.** *Free Radic Biol Med* 2005, **38:**1543–1552.
36. Woodman PG: **p97, a protein coping with multiple identities.** *J Cell Sci* 2003, **116:**4283–4290.
37. Wang HF, Shih YT, Chen CY, Chao HW, Lee MJ, Hsueh YP: **Valosin-containing protein and neurofibromin interact to regulate dendritic spine density.** *J Clin Invest* 2011, **121:**4820–4837.
38. Cooper AJL: **^{13}N as a tracer for studying glutamate metabolism.** *Neurochem Int* 2011, **59:**456–464.
39. Ohnuki M, Takahashi N, Yamasaki M, Fukui T: **Different localization in rat brain of the novel cytosolic ketone body-utilizing enzyme, acetoacetyl-CoA synthetase, as compared to succinyl-CoA:3 –oxoacid CoA-transferase.** *Biochim Biophys Acta* 2005, **1729:**147–153.
40. Das SK, Hiran KR, Mukherjee S, Vasudevan DM: **Oxidative stress is the primary event: effects of ethanol consumption in brain.** *Indian J Clin Biochem* 2007, **22:**99–104.
41. Murphey RK, Godenschwege TA: **New roles for ubiquitin in the assembly and function of neuronal circuits.** *Neuron* 2002, **36:**5–8.
42. Artal-Sanz M, Tavernarakis N: **Prohibitin couples diapause signalling to mitochondrial metabolism during ageing in *C.elegans*.** *Nature* 2009, **461:**793–797.
43. Merkwirth C, Langer T: **Prohibitin function within mitochondria: essential roles for cell proliferation and cristae morphogenesis.** *Biochim Biophys Acta* 2009, **1793:**27–32.
44. Mishra S, Ande SR, Nyomba BL: **The role of prohibitin in cell signaling.** *FEBS J* 2010, **277:**3937–3946.
45. Zhou P, Qian L, D'Aurelio M, Cho S, Wang G, Manfredi G, Pickel V, Iadecola C: **Prohibitin reduces mitochondrial free radical production and protects brain cells from different injury modalities.** *J Neurosci* 2012, **32:**583–592.
46. Tsujita K, Itoh T, Kondo A, Oyama M, Kozuka-Hata H, Irino Y, Hasegawa J, Takenawa T: **Proteome of acidic phospholipid-binding proteins: spatial and temporal regulation of coronin 1A by phosphoinositides.** *J Biol Chem* 2010, **285:**6781–6789.
47. Tada T, Simonetta A, Batterton M, Kinoshita M, Edbauer D, Sheng M: **Role of septin cytoskeleton in spine morphogenesis and dendrite development in neurons.** *Curr Biol* 2007, **17:**1752–1758.
48. Traudt CM, Tkac I, Ennis KM, Sutton LM, Mammel DM, Rao R: **Postnatal morphine administration alters hippocampal development in rats.** *J Neurosci Res* 2012, **90:**307–314.
49. Plafker SM, Macara IG: **Ribosomal protein L12 uses a distinct nuclear import pathway mediated by importin 11.** *Mol Cell Biol* 2002, **22:**1266–1275.
50. Filizola M, Devi LA: **Structural biology: how opiod drugs bind to receptors.** *Nature* 2012, **485:**314–317.
51. Manglik A, Kruse AC, Kobilka TS, Thian FS, Mathiesen JM, Sunahara RK, Pardo L, Weis WI, Kobilka BK, Granier S: **Crystal structure of the μ-opioid receptor bound to a morphinan antagonist.** *Nature* 2012, **485:**321–326.
52. Sim LJ, Selley DE, Dworkin SI, Childers SR: **Effects of chronic morphine administration on μ opioid receptor-stimulated [^{35}S]GTPγS autoradiography in rat brain.** *J Neurosci* 1996, **16:**2684–2692.

53. Maher CE, Martin TJ, Childers SR: **Mechanisms of mu opioid receptor/G-protein desensitization in brain by chronic heroin administration.** *Life Sci* 2005, **77:**1140–1154.
54. Sim-Selley LJ, Selley DE, Vogt LJ, Childers SR, Martin TJ: **Chronic heroin self-administration desensitizes μ opioid receptor-activated G-proteins in specific regions of rat brain.** *J Neurosci* 2000, **20:**4555–4562.
55. Bierczynska-Krzysik A, Bonar E, Drabik A, Noga M, Suder P, Dylag T, Dubin A, Kotlinska J, Silberring J: **Rat brain proteome in morphine dependence.** *Neurochem Int* 2006, **49:**401–406.
56. Bierczynska-Krzysik A, Pradeep John JP, Silberring J, Kotlinska J, Dylag T, Cabatic M, Lubec G: **Proteomic analysis of rat cerebral cortex, hippocampus and striatum after exposure to morphine.** *Int J Mol Med* 2006, **18:**775–784.
57. Bodzon-Kułakowska A, Suder P, Mak P, Bierczynska-Krzysik A, Lubec G, Walczak B, Kotlinska J, Silberring J: **Proteomic analysis of striatal neuronal cell cultures after morphine administration.** *J Sep Sci* 2009, **32:**1200–1210.
58. Drastichova Z, Bourova L, Hejnova L, Jedelsky P, Svoboda P, Novotny J: **Protein alterations induced by long-term agonist treatment of HEK293 cells expressing thyrotropin-releasing hormone receptor and $G_{11}\alpha$ protein.** *J Cell Biochem* 2010, **109:**255–264.
59. Kraus MA, Piper JM, Kornetsky C: **Persistent increases in basal cerebral metabolic activity induced by morphine sensitization.** *Pharmacol Biochem Behav* 1997, **57:**89–100.
60. Magistretti PJ, Pellerin L: **Cellular mechanisms of brain energy metabolism and their relevance to functional brain imaging.** *Philos Trans R Soc Lond B Biol Sci* 1999, **354:**1155–1163.
61. Magistretti PJ, Allaman I: **Glycogen: a Trojan horse for neurons.** *Nat Neurosci* 2007, **10:**1341–1342.
62. Guzman DC, Vazquez IE, Brizuela NO, Alvarez RG, Mejia GB, Garcia EH, Santamaria D, La Rosa De Apreza M, Olguin HJ: **Assessment of oxidative damage induced by acute doses of morphine sulfate in postnatal and adult rat brain.** *Neurochem Res* 2006, **31:**549–554.
63. Matousek P, Novotny J, Svoboda P: **Resolution of G(s)alpha and G(q)alpha/G(11)alpha proteins in membrane domains by two-dimensional electrophoresis: the effect of long-term agonist stimulation.** *Physiol Res* 2004, **53:**295–303.
64. Matousek P, Novotny J, Rudajev V, Svoboda P: **Prolonged agonist stimulation does not alter the protein composition of membrane domains in spite of dramatic changes induced in a specific signaling cascade.** *Cell Biochem Biophys* 2005, **42:**21–40.
65. Moravcova Z, Rudajev V, Stohr J, Novotny J, Cerny J, Parenti M, Milligan G, Svoboda P: **Long-term agonist stimulation of IP prostanoid receptor depletes the cognate G(s)alpha protein in membrane domains but does not change the receptor level.** *Biochim Biophys Acta* 2004, **1691:**51–65.
66. Gharahdaghi F, Weinberg CR, Meagher DA, Imai BS, Mische SM: **Mass spectrometric identification of proteins from silver-stained polyacrylamide gel: a method for the removal of silver ions to enhance sensitivity.** *Electrophoresis* 1999, **20:**601–605.
67. Shevchenko A, Wilm M, Vorm O, Mann M: **Mass spectrometric sequencing of proteins from silver-stained polyacrylamide gels.** *Anal Chem* 1996, **68:**850–858.
68. Sinha P, Poland J, Schnölzer M, Rabilloud T: **A new silver staining apparatus and procedure for matrix-assisted laser desorption/ionization-time of flight analysis of proteins after two-dimensional electrophoresis.** *Proteomics* 2001, **1:**835–840.
69. Fountoulakis M, Takács MF, Berndt P, Langen H, Takács B: **Enrichment of low abundance proteins of Escherichia coli by hydroxyapatite chromatography.** *Electrophoresis* 1999, **20:**2181–2195.
70. Shevchenko A, Tomas H, Havlis J, Olsen JV, Mann M: **In-gel digestion for mass spectrometric characterization of proteins and proteomes.** *Nat Protoc* 2006, **1:**2856–2860.

doi:10.1186/1477-5956-12-11
Cite this article as: Ujcikova *et al.*: Proteomic analysis of post-nuclear supernatant fraction and percoll-purified membranes prepared from brain cortex of rats exposed to increasing doses of morphine. *Proteome Science* 2014 **12**:11.

Physiol. Res. 63 (Suppl. 1): S165-S176, 2014

REVIEW

Opioid-Receptor (OR) Signaling Cascades in Rat Cerebral Cortex and Model Cell Lines: the Role of Plasma Membrane Structure

H. UJČÍKOVÁ[1], J. BREJCHOVÁ[1], M. VOŠAHLÍKOVÁ[1], D. KAGAN[1], K. DLOUHÁ[1], J. SÝKORA[2], L. MERTA[1], Z. DRASTICHOVÁ[3], J. NOVOTNÝ[3], P. OSTAŠOV[1], L. ROUBALOVÁ[1], M. PARENTI[4], M. HOF[2], P. SVOBODA[1]

[1]Department of Biochemistry of Membrane Receptors, Institute of Physiology Academy of Sciences of the Czech Republic, Prague, Czech Republic, [2]J. Heyrovský Institute of Physical Chemistry, Academy of Sciences of the Czech Republic, Prague, Czech Republic, [3]Department of Physiology, Faculty of Sciences, Charles University, Prague, Czech Republic, [4]Department of Experimental Medicine, University of Milano-Bicocca, Monza, Italy

Received August 9, 2013
Accepted August 15, 2013

Summary

Large number of extracellular signals is received by plasma membrane receptors which, upon activation, transduce information into the target cell interior *via* trimeric G-proteins (GPCRs) and induce activation or inhibition of adenylyl cyclase enzyme activity (AC). Receptors for opioid drugs such as morphine (μ-OR, δ-OR and κ-OR) belong to rhodopsin family of GPCRs. Our recent results indicated a specific up-regulation of AC I (8-fold) and AC II (2.5-fold) in plasma membranes (PM) isolated from rat brain cortex exposed to increasing doses of morphine (10-50 mg/kg) for 10 days. Increase of ACI and ACII represented the specific effect as the amount of ACIII-ACIX, prototypical PM marker Na, K-ATPase and trimeric G-protein α and β subunits was unchanged. The up-regulation of ACI and ACII faded away after 20 days since the last dose of morphine. Proteomic analysis of these PM indicated that the brain cortex of morphine-treated animals cannot be regarded as being adapted to this drug because significant up-regulation of proteins functionally related to oxidative stress and alteration of brain energy metabolism occurred. The number of δ-OR was increased 2-fold and their sensitivity to monovalent cations was altered. Characterization of δ-OR-G-protein coupling in model HEK293 cell line indicated high ability of lithium to support affinity of δ-OR response to agonist stimulation. Our studies of PM structure and function in context with desensitization of GPCRs action were extended by data indicating participation of cholesterol-enriched membrane domains in agonist-specific internalization of δ-OR. In HEK293 cells stably expressing δ-OR-$G_i1α$ fusion protein, depletion of PM cholesterol was associated with the decrease in affinity of G-protein response to agonist stimulation, whereas maximum response was unchanged. Hydrophobic interior of isolated PM became more "fluid", chaotically organized and accessible to water molecules. Validity of this conclusion was supported by the analysis of an immediate PM environment of cholesterol molecules in living δ-OR-$G_i1α$-HEK293 cells by fluorescent probes 22- and 25-NBD-cholesterol. The alteration of plasma membrane structure by cholesterol depletion made the membrane more hydrated. Understanding of the positive and negative feedback regulatory loops among different OR-initiated signaling cascades (μ-, δ-, and κ-OR) is crucial for understanding of the long-term mechanisms of drug addiction as the decrease in functional activity of μ-OR may be compensated by increase of δ-OR and/or κ-OR signaling.

Key words

GPCR • Morphine • μ-, δ- and κ-opioid receptors • Rat brain cortex • Adenylyl cyclase I and II • Proteomic analysis • Monovalent cations • Agonist-induced internalization • Plasma membrane structure • Cholesterol • Membrane domains • Fluorescent probes

Corresponding author

P. Svoboda, Institute of Physiology, v.v.i., Academy of Sciences of the Czech Republic, Vídeňská 1083, CZ-142 20 Prague 4, Czech Republic. E-mail: svobodap@biomed.cas.cz

Introduction

Hormones, neurotransmitters and growth factors bind to the cell surface membrane receptors, which may be divided into the three main families: i) coupled with guanine nucleotide-binding regulatory proteins (GPCR), ii) ionic channels, and iii) tyrosine-kinases. Binding of hormones or neurotransmitters to the stereo-specific site of receptor molecules located at extracellular side of plasma membrane represents the first step in complicated sequence of molecular events transmitting the signal into the cell interior and initiating the ultimate physiological response. In G-protein-mediated cascades, ligand binding induces conformational change of receptor molecule, which, in the next step, induces dissociation of trimeric G-protein complex (non-active) into the free, active Gα and Gβγ subunits. Subsequently, both Gα and Gβγ subunits activate variety of enzyme activities and/or ionic channels which regulate intracellular concentrations of secondary messengers such as cAMP, cGMP, IP_3, DAG, arachidonic acid, sodium, potassium or calcium cations (Svoboda *et al.* 2004, Drastichova *et al.* 2008).

Receptors for opioid drugs, μ-OR, δ-OR and κ-OR, were classified as members of rhodopsin family of GPCRs. All these receptors are known to inhibit adenylyl cyclase activity in pertussis-toxin-dependent manner by activation of G_i/G_o class of trimeric G-proteins. These proteins (G_i1, G_i2, G_i3, G_o1, G_o2) are present in brain in large quantities and inhibit adenylyl cyclase activity or regulate ionic channels in pertussis-toxin-dependent manner.

Morphine binds to all three types of OR (μ-, δ- and κ-OR) and represents one of the most effective painkillers. Repeated exposure of experimental animals to morphine results in tolerance to this drug, development of physical dependence and a chronic relapsing disorder – drug addiction (Contet *et al.* 2004). Physical dependence contributes to a drug seeking behavior and the continuous drug use with the aim to prevent the onset of unpleasant withdrawal symptoms (Preston *et al.* 1991). Morphine withdrawal generates a set of symptoms like retches, vomiting, blood pressure increase, insomnia, intestines dysfunctions, body shaking and teeth chatter.

Drug addiction to morphine is characterized by a complex etiology including changes in psychology of experimental animals as well as physiology of their brain function. These changes proceed mainly in the brainstem and hippocampus (Connor and Christie 1999, Law *et al.* 2000, 2004, Chen *et al.* 2007). However, some of the long-term behavioral consequences of repeated morphine exposure were related to reorganized patterns of synaptic connectivity in the forebrain (Robinson *et al.* 1999). Morphine-induced changes of brain function were also associated with alterations of neurotransmission, specific signaling cascades, energy metabolism and stability of protein molecules (Miller *et al.* 1972, Kim *et al.* 2005, Li *et al.* 2006, Li *et al.* 2009)

Hyper-sensitization or super-activation of adenylyl cyclase (AC) activity by prolonged exposure of cultured cells or mammalian organism to morphine has been demonstrated in previous studies delineating the mechanism of action of this drug (Preston 1991, Connor and Christie 1999, Law *et al*. 2000, 2004, Contet *et al.* 2004) and considered as biochemical basis for development of opiate tolerance and dependence.

Our previous work on PM fraction isolated from brain cortex in Percoll gradient of rats exposed to morphine for 10 days (10-50 mg/kg) indicated a desensitization of G-protein response to μ-OR (DAMGO) and δ-OR (DADLE) stimulation (Bourova *et al.* 2009, 2010) and specific increase of ACI (8-fold) and ACII (2.5-fold) isoforms (Ujcikova *et al.* 2011). The κ-OR (U-23554)-stimulated [^{35}S]GTPγS binding and expression level of ACIII-IX in PM was unchanged. Behavioral tests of morphine-treated animals indicated that these animals were fully drug-dependent (opiate abstinence syndrome) and developed tolerance to subsequent drug addition (analgesic tolerance detected by hot-plate and hind paw withdrawal tests). The increase of ACI and ACII was interpreted as a specific compensatory response to prolonged stimulation of brain cortex OR by morphine.

Proteomic analysis of membrane proteins in rat brain cortex: changes induced by the long-term exposure to increasing doses to morphine

The aim of the next step of our work was the description of an overall change of membrane protein composition and recognition of proteins exhibiting the largest changes induced by morphine. This was performed by proteomic analysis of post-nuclear supernatant (PNS) and plasma membrane-enriched fraction isolated in Percoll gradient. PNS was analyzed because it contains proteins of mitochondrial, endoplasmic reticulum, plasma membrane and cytoplasmic origin. Rats were adapted to morphine for

10 days [10 mg/kg (day 1 and 2), 15 mg/kg (day 3 and 4), 20 mg/kg (day 4 and 5), 30 mg/kg (day 6 and 7), 40 mg/kg (day 9) and 50 mg/kg (day 10)] and sacrificed 24 h after the last dose (group +M10). Control animals were sacrificed in parallel with morphine-treated (group −M10). Post-nuclear supernatant fraction was prepared from brain cortex of both groups and resolved by 2D-ELFO. The gels were stained by Coomassie brilliant blue (CBB) and the altered proteins detected by PDQuest software analysis.

The 10 up-regulated or down-regulated proteins exhibiting the largest morphine-induced change were selected, excised manually from 2D-gel and identified by MALDI-TOF MS/MS. The identified proteins were: 1) (gi|148747414, Guanine deaminase), up 2.5-fold; 2) (gi|17105370, Vacuolar-type proton ATP subunit B, brain isoform), up 2.6-fold; 3) (gi|1352384, Protein disulfide-isomerase A3), up 3.4-fold; 4) (gi|40254595, Dihydropyrimidinase-related protein 2), up 3.6-fold; 5) (gi|149054470, N-ethylmaleimide sensitive fusion protein, isoform CRAa), up 2.0-fold; 6) (gi|42476181, Malate dehydrogenase, mitochondrial precursor), up 1.4-fold; 7) (gi|62653546, Glyceraldehyde-3-phosphate dehydrogenase), up 1.6-fold; 8) (gi|202837, Aldolase A), up 1.3-fold; 9) (gi|31542401, Creatine kinase B-type), down 0.86-fold; 10) (gi|40538860, Aconitate hydratase, mitochondrial precursor), up 1.3-fold. Thus, the ten most highly altered proteins in PNS were of cytoplasmic (proteins no. 1, 4, 5, 7, 9), cell membrane (protein no. 2), endoplasmic reticulum (protein no. 3) and mitochondrial (proteins no. 6, 8, 10) origin and nine of them were significantly increased by morphine (1.3 to 3.6-fold). Correlation with functional properties of these proteins indicated up-regulation of proteins related to guanine degradation (protein no. 1), vacuolar acidification (protein no. 2), apoptotic cell death (protein no. 3), oxidative stress (proteins no. 4, 6, 7, 10), membrane traffic (protein no. 5) and glycolysis (protein no. 8). The role in apoptosis has been also described for glyceraldehyde-3-phosphate dehydrogenase (protein no. 7), already mentioned as major target protein in oxidative stress (Hwang *et al.* 2009). All together, the spectrum of altered proteins suggests a major change of energy metabolism of brain cortex tissue when exposed to increasing doses of morphine. Judged from functional point of view, the most significant change was the up-regulation of proteins related to oxidative stress (proteins no. 4, 6, 7, 10) and apoptotic cell death (proteins no. 3, 7).

We could therefore conclude that the brain cortex of rats exposed to increasing doses of morphine (10-50 mg/kg) for 10 days cannot be regarded as being adapted to this drug. Significant up-regulation of proteins functionally related to oxidative stress and apoptosis indicates the state of severe "discomfort" of brain cells or even damage.

Identification of an active, minority pool of trimeric Gβ subunits responding to chronic morphine in rat brain cortex: proteomic analysis of Percoll-purified membranes

In PM, the altered proteins were of plasma membrane origin [BASP1, Brain acid soluble protein, down-regulated 2.1-fold; GBB, Guanine nucleotide-binding protein subunit beta-1, down 2.0-fold], myelin membrane [MBP, Myelin basic protein S, down 2.5-fold], cytoplasmic [KCRB, Creatine kinase B-type (EC 2.7.3.2), down 2.6-fold; AINX, alpha-internexin, up-regulated 5.2-fold; DPYL2, Dihydropyrimidinase-related protein 2, up 4.9-fold; SIRT2, NAD-dependent deacetylase sirtuin-2, up 2.5-fold; SYUA, Alpha-synuclein, up 2.0-fold; PRDX2, Peroxiredoxin-2, up 2.2-fold; TERA, Transitional endoplasmic reticulum ATPase, up 2.1-fold; UCHL1, Ubiquitin carboxyl-terminal hydrolase L1 down 2.0-fold; COR1A, Coronin-1A, down 5.4-fold; SEP11, Septin-11, up 2.2-fold; RL12, 60S ribosomal protein L12, up 2.7-fold] and mitochondrial [DHE3, Glutamate dehydrogenase 1, up 2.7-fold; SCOT1, Succinyl-CoA:3-ketoacid-coenzyme A, up 2.2-fold; AATM, Aspartate aminotransferase, down 2.2-fold; PHB, Prohibitin, up 2.2-fold].

The only member of GPCR-initiated signaling cascades identified by LC-MS/MS in PM was trimeric Gβ subunit (2-GBB) which was decreased 2-fold in samples from morphine-adapted rats. Similarly, proteomic analysis of protein alterations induced by long-term stimulation of HEK293 cells stably expressing TRH-receptor and $G_{11}\alpha$ protein by TRH, indicated the change of 42 proteins, but none of these proteins represented the plasma membrane protein functionally related to G-protein-mediated signaling cascades (Drastichova *et al.* 2010).

The immunoblot analysis of the same PM resolved by 2D-ELFO indicated that the "active" pool of Gβ subunits affected by morphine, which was decreased 2x, represented just a minor fraction of the total signal of Gβ subunits in 2D-gels (Fig. 1). The total signal of Gβ was

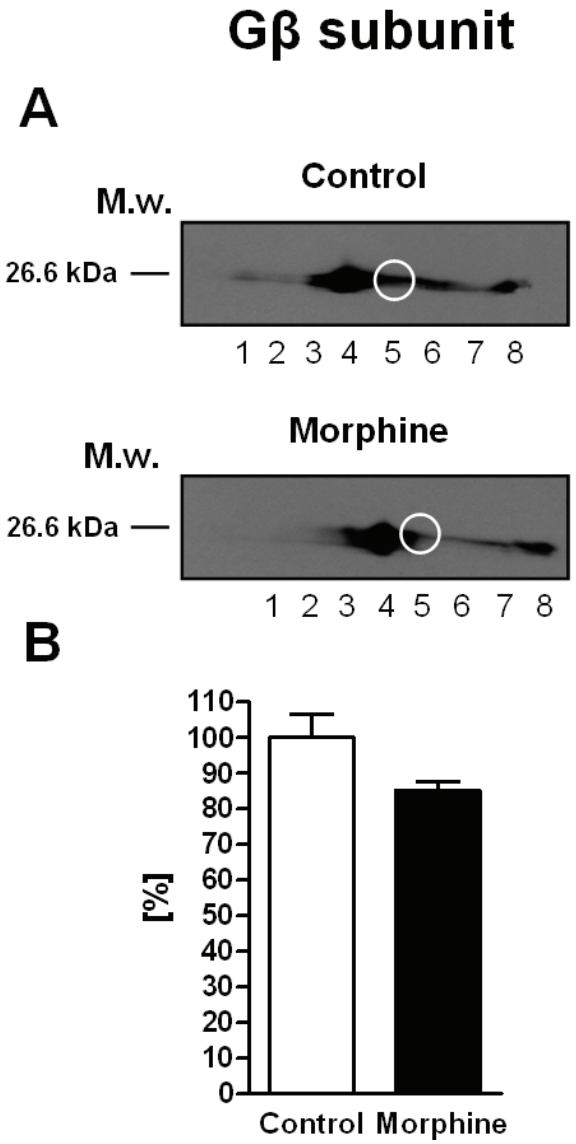

Fig. 1. Morphine-induced decrease of trimeric Gβ subunits in plasma-membrane-enriched fraction: immunoblot analysis of 2D-electrophoresis. **(A)** Two-dimensional resolution of Gβ protein content in PM isolated from control and morphine-adapted rats. PM protein (400 μg) was resolved by 2D electrophoresis using the pI range 3-11 for isoelectric focusing in the first dimension. The white small circle shows the small fraction of the total signal of Gβ which was taken into consideration when analyzed by LC-MS/MS. The second dimension was performed by SDS-PAGE in 10 % w/v acrylamide/0.26 % bis-acrylamide gels (Hoefer SE 600). Gβ was identified by immunoblotting with specific antibody oriented against C-terminal peptide of Gβ. Numbers 1-8 represent spots of Gβ subunits which were subsequently analyzed by LC-MS/MS. **(B)** The average of three immunoblots ± SEM. Difference between (-M10) and (+M10) was analyzed by Student´s *t*-test using GraphPad*Prizm4* and found not significant, NS ($p>0.05$).

decreased 1.2-fold only but dominant/major part of the total signal was unchanged. Accordingly, the immunoblot analysis of Gβ after resolution by 1D-SDS-PAGE in 10 % w/v acrylamide/0.26 % w/v bis-acrylamide or 4-12 % (InVitroGene) gradient gels indicated no change of this protein. We could therefore conclude that proteomic analysis represents a valuable tool for identification of membrane proteins. However, the analysis of low-abundance proteins of OR-initiated signaling cascades in plasma membranes has to be accompanied by specific immublot analysis. Identification of an "active", minority pool of Gβ subunits down-regulated by morphine represents an original finding which has not been described in current literature dealing with drug addiction and morphine effect on mammalian brain.

The effect of lithium and other monovalent cations on ligand binding and efficiency of δ-opioid receptor-G-protein coupling

Lithium is still one of the most effective therapies for depression. Comparison of the effect of lithium, sodium and potassium on δ-opioid receptors was studied in HEK293 cells stably expressing PTX-insensitive δ-OR-$G_i1\alpha$ (Cys^{351}-Ile^{351}) fusion protein. δ-OR-$G_i1\alpha$ (C^{351}-I^{351}) cells represent useful experimental tool as the covalent bond between δ-OR and $G_i1\alpha$ (C^{351}-I^{351}) provides the permanent and fixed 1:1 stoichiometry and C^{351}-I^{351} mutation provides resistance to PTX together with extraordinary high efficacy of coupling between δ-OR and $G_i1\alpha$ (C^{351}-I^{351}) protein (Bourova *et al.* 2003, Brejchova *et al.* 2011).

Agonist [^{3}H]DADLE binding was decreased with the order: $Na^+ \gg Li^+ > K^+ > NMDG^+$. When plotted as a function of increasing NaCl concentrations, binding was best-fitted with a two phase exponential decay considering the two Na^+-responsive sites ($r^2=0.99$). High-affinity Na^+-sites were characterized by $K_d=7.9$ mM and represented 25 % of the basal level determined in the absence of Na^+ ions. Remaining 75 % represented the low-affinity sites ($K_d=463$ mM). Inhibition of [^{3}H]DADLE binding by lithium, potassium and $NMDG^+$ proceeded in low-affinity manner only. Preferential sensitivity of δ-OR-$G_i1\alpha$ to sodium was thus clearly manifested.

Surprisingly, the affinity/potency of DADLE-stimulated [^{35}S]GTPγS binding, quantitatively characterized by comparison of dose-response curves in different ion media (EC_{50} values), was increased in reverse order: $Na^+ < K^+ < Li^+$. This result was demonstrated in PTX-treated as well as PTX-untreated cells (Table 1). Therefore, this finding is not restricted to $G_i1\alpha$ present in fusion protein, but is also valid for stimulation of endogenous G-proteins of G_i/G_o family.

Table 1. DADLE-stimulated [^{35}S]GTPγS binding in membranes prepared from PTX-treated and PTX-untreated δ-OR-$G_i1\alpha$ - HEK293 cells.

A PTX-treated

	EC_{50}		%		B_{basal}		B_{max}		Δ_{max}	
NaCl	5.1×10^{-8} M	**	350	**	0.143	**	0.499	*	0.356	**
KCl	9.6×10^{-9} M	* **	216	NS **	0.241	NS **	0.520	** NS	0.279	NS **
LiCl	5.4×10^{-9} M		231		0.209		0.481		0.272	

B PTX-untreated

	EC_{50}		%		B_{basal}		B_{max}		Δ_{max}	
NaCl	6.5×10^{-8} M	**	327	*	0.178	**	0.582	*	0.404	**
KCl	2.0×10^{-8} M	* **	237	NS *	0.222	NS **	0.526	NS *	0.304	NS **
LiCl	8.4×10^{-9} M		248		0.211		0.523		0.312	

[^{35}S]GTPγS binding was measured in P2 membrane fraction isolated from PTX-treated **(A)** or PTX-untreated cells **(B)** as described in methods. Binding assays were performed in 200 mM NaCl, KCl or LiCl. EC_{50} (M) and B_{max} (pmol x mg^{-1}) values were calculated by GraphPad*Prizm4*. B_{max} values were also expressed as the ratio (%) between maximum DADLE-stimulated (B_{max}) and the basal level (B_{basal}) of binding. Net-increment of agonist stimulation (Δ_{max}) was calculated as the difference between B_{max} and B_{basal} values. Numbers represent the means ± SEM of 3 binding assays, each performed in triplicates. Data were analyzed by one-way ANOVA followed by Neuman-Keuls post test (* $p<0.05$, ** $p<0.01$, NS non-significant). **(A)** In PTX-treated membranes, [^{35}S]GTPγS binding in the absence of ions was 0.622 pmol × mg^{-1} and this level was decreased to 0.143 (NaCl), 0.241 (KCl) and 0.209 (LiCl) pmol × mg^{-1} by addition of 200 mM NaCl, KCl or LiCl, respectively. **(B)** In PTX-untreated membranes, [^{35}S]GTPγS binding in the absence of ions was 0.809 pmol × mg^{-1} and this level was decreased to 0.178 (NaCl), 0.222 (KCl) and 0.211 (LiCl) pmol × mg^{-1} by addition of 200 mM NaCl, KCl or LiCl, respectively.

This surprising but fully reproducible result may be considered in connection with clinical use of lithium in the treatment of manic depression. In electrically active cells, Li^+ enters the intracellular compartment *via* "fast" sodium channel (Richelson, 1977) and also *via* ouabain-sensitive K^+-influx catalyzed by Na,K-ATPase. However, the efflux of Li^+ *via* Na,K-ATPase is limited because ATP+Mg+Na-dependent phosphorylation proceeding at inner side of the plasma membrane and outward oriented efflux of Na^+ cations *via* Na+-pump are strictly specific for sodium. Thus, if available in extracellular space, the intracellular Li^+ concentration will be slowly increased. It is reasonable to assume that such conditions may arise in neuronal or glial cells of depressive patients as the effective range of plasma Li^+ concentrations under clinical conditions is 0.6-1.0 mM. The 2 mM LiCl is regarded as toxic. This is exactly the concentration range in which the first significant inhibition of the basal level of [^{35}S]GTPγS binding was detected in our experiments. The first significant decrease of the basal level of [^{35}S]GTPγS binding measured in the absence of cations was noticed at 1-2 mM NaCl, KCl and LiCl; the 50 % inhibition was reached at 62 mM NaCl, 88 mM LiCl and 92 mM KCl, respectively (Vosahlikova and Svoboda 2011). Thus, in the treatment of acute depression, competitive effect of Li^+ on inverse agonist-like effect of Na^+ on δ-OR and, in parallel, on G_i/G_o class of G-proteins, might be considered as one of plausible mechanisms of Li^+ action besides its numerous other effects on overall cell metabolism (Young 2009).

The role of cholesterol, cholesterol depletion and membrane domains/rafts in structural organization of plasma membrane and transmembrane signaling through G-protein-coupled receptors

Cholesterol constitutes a major component of mammalian plasma (cell) membrane. Its correct distribution among plasma membrane and intracellular membrane compartments is essential for the homeostasis of mammalian cells and intracellular membrane traffic plays a major role in the correct disposition of internalized cholesterol and in the regulation of cholesterol efflux (Maxfield and Wüstner 2002, Scheidt *et al.* 2003). Furthermore, lateral and transbilayer organization of cholesterol molecules in the plasma membrane determines plasma membrane structure and dynamics. However, neither its intracellular pathways of trafficking nor its precise lateral organization in cholesterol-enriched microdomains such as membrane rafts and caveolae is fully understood. The same applies to the transbilayer distribution between the two leaflets of biological membranes (Simons and Ikonen 1997, Brown and London 1998, Anderson and Jacobson 2002).

Cholesterol- and sphingolipid-enriched membrane domains, characterized by high content of cholesterol, saturated phospholipids, glycolipids and sphingomyelin, have been described as lipid platforms capable to harbor and confine trimeric G-proteins in high amounts (Simons and Ikonen 1997, Brown and London 1998, Anderson 1998, Moffett *et al.* 2000, Oh and Schnitzer 2001, Anderson and Jacobson 2002, Pike 2004, Quinton *et al.* 2005). Considering the function of trimeric G-proteins in membrane domains containing caveolin, heterologous desensitization of GPCR signaling was described as specific binding of G-proteins to caveolin (Murthy and Makhlouf 2000).

These structures were also reported to play an important role in both positive and negative regulation of transmembrane signaling through G-protein-coupled receptors (Gimpl *et al.* 1995, Klein *et al.* 1995, Feron *et al.* 1997, De Weerd and Leeb-Lundberg 1997, Schwencke *et al.* 1999, De Luca *et al.* 2000, Dessy *et al.* 2000, Lasley *et al.* 2000, Igarashi and Michel 2000, Ostrom *et al.* 2000, 2001, Rybin *et al.* 2000, 2003, Ushio-Fukai *et al.* 2001, Gimpl and Farenholz 2002, Sabourin *et al.* 2002, Ostrom and Insel 2004, Pucadyil and Chattopadhyay 2004, 2007, Monastyrskaya *et al.* 2005, Savi *et al.* 2006, Xu *et al.* 2006, Allen *et al.* 2007, Ostasov *et al.* 2007, 2008, Chini and Parenti 2009). More specifically, the functional significance of OR presence in membrane domains is far from being understood as cholesterol reduction by methyl-β-cyclodextrin attenuated δ-OR-mediated signaling in neuronal cells but enhanced it in non-neuronal cells (Huang *et al.* 2007).

In HEK293 cells stably expressing δ-OR-$G_i1α$ fusion protein, depletion of PM cholesterol was associated with a decrease (by one order of magnitude) in affinity/potency of G-protein response to agonist stimulation. The maximum response was unchanged (Brejchova *et al.* 2011). Hydrophobic interior of isolated PM became more "fluid", chaotically organized and more accessible to water molecules. The analysis of PM environment by fluorescent derivatives of cholesterol (22- and 25-NBD-cholesterol) in living δ-OR-$G_i1α$-HEK293 cells confirmed these results because the alteration of plasma membrane structure by cholesterol depletion made the membrane more hydrated (Ostasov *et al.* 2013). Our data also indicated that small perturbation of PM structure by low, non-ionic detergent concentrations increased GPCR-G-protein coupling, while the high concentrations were strictly inhibitory (Sykora *et al.* 2009). The close-to-zero level of basal and agonist-stimulated G-protein activity is the typical feature of detergent-resistant membrane domains (DRMs) prepared at high detergent concentrations, 0.5-1 % Triton X-100 (Bourova *et al.* 2003).

Agonist-induced internalization of δ-opioid receptors

The first evidence for agonist-induced internalization of GPCRs was brought by subcellular fractionation studies of cell homogenate using differential or sucrose density gradient centrifugation. The internalized, endosomal pool of receptor molecules was separated from the major pool of receptor molecules in plasma membranes and was found to be increased by agonist stimulation (Stadel *et al.* 1983, Waldo *et al.* 1983, Clark *et al.* 1985, Hertel *et al.* 1985, Sibley *et al.* 1987). In intact cells, the specific, agonist-induced sequestration and internalization of GPCRs was detected by immunofluorescence microscopy of cells expressing $β_2$-adrenergic receptors. $β_2$-AR were transferred from clathrine-coated pitts (in the plasma membrane) to clathrine-coated vesicles, rab5-containing early endosomes and back to the plasma membrane (von Zastrow and Kobilka 1992, 1994, Moore *et al.* 1995,

Pippig *et al.* 1995). Cellular and molecular mechanisms of GPCR internalization are in focus of OR studies as one the leading theories of drug addiction is directly based on atypical parameters of μ-OR internalization (Whistler and von Zastrow 1998, Whistler *et al.* 1999). When exposed to morphine, μ-OR remain at PM and in this way elude desensitization by β-arrestin.

Our analysis of HEK293 cells transiently expressing Flag-epitope tagged version of δ-OR indicated that cholesterol depletion alone induced transfer of receptor molecules into the cell interior (Fig. 2A, upper right and left panels). Incubation of cells with 10 mM β-cyclodextrin (β-CDX, 30 min) caused significant increase of intracellular fluorescence ($p<0.05$), while in control, β-CDX-untreated cells, the small intracellular signal distributed among numerous faint fluorescent patches was unchanged in the course of 30 min incubation in serum-free medium alone (Fig. 2B). Massive transfer of receptor molecules from the cell surface (plasma membrane) into the intracellular compartments was noticed after agonist stimulation (100 nM DADLE). This transfer was decreased in β-CDX-treated cells (Fig. 2A, lower right and left panels). Difference between β-CDX-treated and β-CDX-plus DADLE-treated samples was highly significant ($p<0.01$) (Fig. 2B).

We could therefore conclude that the treatment of HEK293 cells with β-CDX alone, i.e. degradation of membrane domains, induced destabilization of HEK293 plasma membrane structure manifested as spontaneous transfer of a portion of δ-OR molecules into the cell interior. Massive internalization of δ-OR proceeding in the presence of specific agonist was suppressed by β-CDX. This part of internalized receptor molecules may be regarded as functionally related to membrane domains.

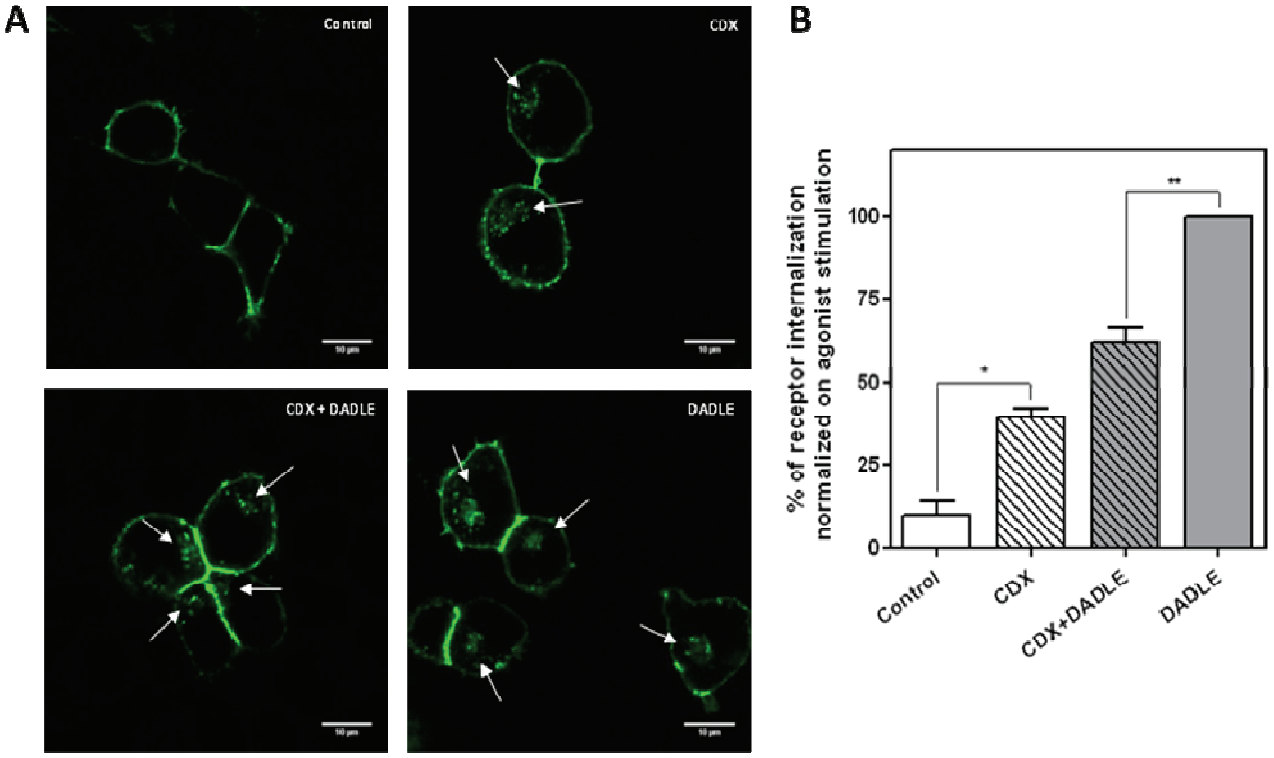

Fig. 2. Agonist (DADLE)-induced internalization of δ-OR is attenuated by cholesterol depletion. HEK293T cells transiently transfected with FLAG-tagged δ-OR were *in vivo* labeled with the corresponding anti-tag antibodies, exposed to serum-free DMEM (Control), 10 mM β-CDX in serum-free DMEM (CDX), 100 nM DADLE (DADLE), or 10 mM β-CDX plus 100 nM DADLE in serum-free DMEM (CDX+DADLE) for 30 min, and fixed. After fixation the cells were subjected to indirect immunofluorescence with Alexa Fluor 488-conjugated secondary antibodies and imaged with laser scanning confocal microscopy. Left panels **(A)** show representative micrographs of cells expressing FLAG-tagged δ-OR and treated as described above. Right panel **(B)** displays results from quantification of micrographs performed by ImageJ software. Fraction of internalized receptors was calculated as a ratio of intracellular to total signal determined in 8 cells per each condition, averaged and normalized to values obtained by agonist (DADLE) stimulation. Data represent the average of three experiments, i.e. three independent transfections, ± SEM. Statistical analysis was performed using one-way ANOVA repeated measurements with Bonferroni *post-hoc* test. *, **, represent the significant difference, $p<0.05$, $p<0.01$.

Conclusions and future perspectives

Understanding of the positive and negative feedback regulatory loops among different OR-initiated signaling cascades (μ-, δ-, and κ-OR) is crucial for understanding of the long-term mechanisms of drug addiction as the decrease in functional activity of μ-OR may be compensated by increase of δ-OR and/or κ-OR signaling. In our experiments using increasing doses of morphine (10-50 mg/kg) for 10 days, the decrease of functional activity of μ-OR in brain cortex PM was measured together with decrease of δ-OR signaling (agonist-stimulated, high-affinity [^{35}S]GTPγS binding). In parallel PM samples, membrane density of adenylyl cyclase I and II was markedly increased; the other AC isoforms (III-IX) were unchanged. The highly positive and "optimistic" result (for drug addicts) was that the up-regulation of ACI and ACII faded away 20 days since the last dose of morphine.

Rat brain cortex of rats sacrificed 24 h after the last dose of morphine (50 mg/kg) cannot be regarded as "being adapted" as the proteomic analysis suggests a major alteration/reorganization of energy metabolism of brain cortex cells: four out of nine up-regulated proteins were described as functionally related to oxidative stress; the two proteins were related to genesis of apoptotic cell death. This was not an optimistic finding indeed (for drug addicts), however, further research is needed to find out whether these changes are reversible as the up-regulation of ACI and ACII after 20 days of drug withdrawal.

Analysis of model HEK293 cell line expressing the defined type of OR (δ-OR) indicated that degradation of membrane domains/rafts by cholesterol depletion resulted in decrease of affinity of δ-OR-response to agonist stimulation in parallel with increase of "fluidity" and hydration of PM. Agonist binding to δ-OR was unchanged. Perturbation of optimum PM organization by cholesterol depletion deteriorated the functional coupling between δ-OR and G-proteins while receptor ligand binding site was unchanged. Therefore, the biophysical state of hydrophobic PM interior should be regarded as regulatory factor of δ-OR-signaling cascade.

In HEK293 cells expressing δ-OR-$G_i1\alpha$ (Cys^{351}-Ile^{351}) fusion protein, the inverse agonist-like effect of monovalent cations on δ-OR was detected as inhibition of agonist binding. Maximum of G-protein response to agonist stimulation was preferentially oriented to sodium with the order: $Na^+ \gg Li^+ > K^+ > NMDG^+$. Surprisingly, affinity of G-protein response was preferentially supported by lithium.

Modern biophysical and confocal microscopy techniques (fluorescence lifetime imaging, fluorescence resonance energy transfer, raster image correlation spectroscopy) are being introduced at present time for the analysis of agonist-induced change of receptor mobility in HEK293 cell lines transiently expressing δ-OR-CFP, δ-OR-YFP and δ-OR-CFP plus δ-OR-YFP. Stably transfected HEK293 cells expressing TRH-R-eGFP and fluorescence recovery after photobleaching are used as reference standard when testing agonist-specific alteration of receptor mobility in living cells.

Conflict of Interest

There is no conflict of interest.

Acknowledgements

This work was supported by Grant Agency of the Czech Republic (P207/12/0919, P304/12/G069) and by the Academy of Sciences of the Czech Republic (RVO:67985823).

References

ALLEN JA, HALVERSON-TAMBOLI RA, RASENICK MM: Lipid raft microdomains and neutrotransmitter signaling. *Nat Rev Neurosci* **8**: 128-140, 2007.

ANDERSON RGW, JACOBSON K: A role for lipid shells in targeting proteins to caveolae, rafts, and other lipid domains. *Science* **296**: 1821-1825, 2002.

ANDERSON RGW: The caveolae membrane system. *Annu Rev Biochem* **67**: 199-225, 1998.

BOUROVA L, KOSTRNOVA A, HEJNOVA L, MORAVCOVA Z, MOON HE, NOVOTNY J, MILLIGAN G, SVOBODA P: delta-Opioid receptors exhibit high efficiency when activating trimeric G proteins in membrane domains. *J Neurochem* **85**: 34-49, 2003.

BOUROVA L, STOHR J, LISY V, RUDAJEV V, NOVOTNY J, SVOBODA P: G-protein activity in Percoll-purified plasma membranes, bulk plasma membranes and low-density plasma membranes isolated from rat cerebral cortex. *Med Sci Monit* **15**: BR111-BR122, 2009.

BOUROVA L, VOSAHLIKOVA M, KAGAN D, DLOUHA K, NOVOTNY J, SVOBODA P: Long-term adaptation to high doses of morphine causes desensitization of μ-OR- and δ-OR-stimulated G-protein response in forebrain cortex but does not decrease the amount of G-protein alpha subunit. *Med Sci Monit* **16**: 260-270, 2010.

BREJCHOVA J, SÝKORA J, DLOUHA K, ROUBALOVA L, OSTASOV P, VOSAHLIKOVA M, HOF M, SVOBODA P: Fluorescence spectroscopy studies of HEK293 cells expressing DOR-Gi1α fusion protein; the effect of cholesterol depletion. *Biochim Biophys Acta* **1808**: 2819-2829, 2011.

BROWN DA, LONDON E: Functions of lipid rafts in biological membranes. *Annu Rev Cell Dev Biol* **14**: 111-136, 1998.

CHEN XL, LU G, GONG YX, ZHAO LC, CHEN J, CHI ZQ, YANG YM, CHEN Z, LI QL, LIU JG: Expression changes of hippocampal energy metabolism enzymes contribute to behavioural abnormalities during chronic morphine treatment. *Cell Res* **17**: 689-700, 2007.

CHINI B, PARENTI M: G-protein-coupled receptors, cholesterol and palmitoylation: facts about fats. *J Mol Endocrinol* **42**: 371-379, 2009.

CLARK RB, FRIEDMAN J, PRASHAD N, RUOHO AE: Epinephrine-induced sequestration of the beta-adrenergic receptor in cultured S49 WT and cyc- lymphoma cells. *J Cyclic Nucleotide Protein Phosphor Res* **10**: 97-119, 1985.

CONNOR M, CHRISTIE MD: Opioid receptor signaling mechanisms. *Clin Exp Pharmacol Physiol* **26**: 493-499, 1999.

CONTET C, KIEFFER BL, BEFORT K: Mu opioid receptor: a gateway to drug addiction. *Curr Opin Neurobiol* **14**: 370-378, 2004.

DE LUCA A, SARGIACOMO M, PUCA A, SGARAMELLA G, DE PAOLIS P, FRATI G, MORISCO C, TRIMARCO B, VOLPE M, CONDORELLI G: Characterization of caveolae from rat heart: localization of postreceptor signal transduction molecules and their rearrangement after norepinephrine stimulation. *J Cell Biochem* **77**: 529-539, 2000.

DE WEERD WFC, LEEB-LUNDBERG LMF: Bradykinin sequesters B2 bradykinin receptors and the receptor-coupled Galpha subunits Galphaq and Galphai in caveolae in DDT1 MF-2 smooth muscle cells. *J Biol Chem* **272**: 17858-17866, 1997.

DESSY C, KELLY RA, BALLIGAND JL, FERON O: Dynamin mediates caveolar sequestration of muscarinic cholinergic receptors and alternation in NO signaling. *EMBO J* **19**: 4272-4280, 2000.

DRASTICHOVA Z, BOUROVA L, LISY V, HEJNOVA L, RUDAJEV V, STOHR, J, DURCHANKOVA D, OSTASOV P, TEISINGER J, SOUKUP T, NOVOTNY J, SVOBODA P: Subcellular redistribution of trimeric G-proteins – potential mechanism of desensitization of hormone response; internalization, solubilisation, down-regulation. *Physiol Res* **57** (Suppl 3): S1-S10, 2008.

DRASTICHOVA Z, BOUROVA L, HEJNOVA L, JEDELSKY P, SVOBODA P, NOVOTNY J: Protein alterations induced by long-term agonist treatment of HEK293 cells expressing thyrotropin-releasing hormone receptor and $G_{11}\alpha$ protein. *J Cell Biochem* **109**: 255-264, 2010.

FERON O, SMITH TW, MICHEL T, KELLY RA: Dynamic targeting of the agonist-stimulated m2 muscarinic acetylcholine receptor to caveolae in cardiac myocytes. *J Biol Chem* **272**: 17744-17748, 1997.

GIMPL G, KLEIN U, REILÄNDER H, FAHRENHOLZ F: Expression of the human oxytocin receptor in baculovirus-infected insect cells: high-affinity binding is induced by a cholesterol-cyclodextrin complex. *Biochemistry* **34**: 13794-13801, 1995.

GIMPL G, FAHRENHOLZ F: Cholesterol as stabilizer of the oxytocin receptor. *Biochim Biophys Acta* **1564**: 384-392, 2002.

HERTEL C, COULTER SJ, PERKINS JP: A comparison of catecholamine-induced internalization of beta-adrenergic receptors and receptor-mediated endocytosis of epidermal growth factor in human astrocytoma cells. Inhibition by phenylarsine oxide. *J Biol Chem* **260**: 12547-12533, 1985.

HUANG P, XU W, YOON SI, CHEN C, CHONG PLG, LIU-CHEN LY: Cholesterol reduction by methyl-beta-cyclodextrin attenuates the delta opioid receptor-mediated signaling in neuronal cells and enhances it in non-neuronal cells. *Biochem Pharmacol* **73**: 534-549, 2007.

HWANG NR, YIM SH, KIM YM, JEONG J, SONG EJ, LEE Y, CHOI S, LEE KJ: Oxidative modifications of glyceraldehyde-3-phophate dehydrogenase play a key role in its multiple cellular functions. *Biochem J* **423**: 253-264, 2009.

IGARASHI J, MICHEL T: Agonist-modulated targeting of the EDG-1 receptor to plasmalemmal caveolae. eNOS activation by sphingosine 1-phosphate and the role of caveolin-1 in sphingolipid signal transduction. *J Biol Chem* **275**: 32363-32370, 2000.

KIM SY, CHUDAPONGSE N, LEE SM, LEVIN MC, OH JT, PARK HJ, HO IK: Proteomic analysis of phosphotyrosyl proteins in morphine-dependent rat brains. *Brain Res Mol Brain Res* **133**: 58-70, 2005.

KLEIN U, GIMPL G, FAHRENHOLZ F: Alteration of the myometrial plasma membrane cholesterol content with beta-cyclodextrin modulates the binding affinity of the oxytocin receptor. *Biochemistry* **34**: 13784-13793, 1995.

LASLEY RD, NARAYAN P, UITTENBOGAARD A, SMART EJ: Activated cardiac adenosine A(1) receptors translocate out of caveolae. *J Biol Chem* **275**: 4417-4421, 2000.

LAW PY, WONG YH, LOH HH: Molecular mechanisms and regulation of opioid receptor signaling. *Annu Rev Pharmacol Toxicol* **40**: 389-430, 2000.

LAW PY, LOH HH, WEI LN: Insights into the receptor transcription and signaling: implications in opioid tolerance and dependence. *Neuropharmacology* **47**: 300-311, 2004.

LI KW, JIMENEZ CR, VAN DER SCHORS RC, HORNSHAW MP, SCHOFFELMEER ANM, SMIT AB: Intermittent administration of morphine alters protein expression in rat nucleus accumbens. *Proteomics* **6**: 2003-2008, 2006.

LI Q, ZHAO X, ZHONG LJ, YANG HY, WANG Q, PU XP: Effects of chronic morphine treatment on protein expression in rat dorsal root ganglia. *Eur J Pharmacol* **612**: 21-28, 2009.

MAXFIELD FR, WÜSTNER D: Intracellular cholesterol transport. *J Clin Invest* **110**: 891-898, 2002.

MILLER AL, HAWKINS RA, HARRIS RL, VEECH RL: The effects of acute and chronic morphine treatment and of morphine withdrawal on rat brain in vivo. *Biochem J* **129**: 463-469, 1972.

MOFFETT S, BROWN DA, LINDER ME: Lipid-dependent targeting of G proteins into rafts. *J Biol Chem* **275**: 2191-2198, 2000.

MONASTYRSKAYA K, HOSTETTLER A, BUERGI S, DRAEGER A: The NK1 receptor localizes to the plasma membrane microdomains, and its activation is dependent on lipid raft integrity. *J Biol Chem* **280**: 7135-7146, 2005.

MOORE RH, SADOVNIKOFF N, HOFFENBERG S, LIU S, WOODFORD P, ANGELIDES K, TRIAL JA, CARSRUD ND, DICKEY BF, KNOLL BJ: Ligand-stimulated beta 2-adrenergic receptor internalization via the constitutive endocytotic pathway into rab5-containing endosomes. *J Cell Sci* **108**: 2983-2991, 1995.

MURTHY KS, MAKHLOUF GM: Heterologous desensitization mediated by G protein-specific binding to caveolin. *J Biol Chem* **275**: 30211-30219, 2000.

OH P, SCHNITZER JE: Segregation of heterotrimeric G proteins in cell surface microdomains: G(q) binds caveolin to concentrate in caveolae, whereas G(i) and G(s) target lipid rafts by default. *Mol Biol Cell* **12**: 685-698, 2001.

OSTASOV P, BOUROVA L, HEJNOVA L, NOVOTNY J, SVOBODA P: Disruption of the plasma membrane integrity by cholesterol depletion impairs effectiveness of TRH receptor-mediated signal transduction via G(q)/G(11)alpha proteins. *J Recept Signal Transduct Res* **27**: 335-352, 2007.

OSTASOV P, KRUSEK J, DURCHANKOVA D, SVOBODA P, NOVOTNY J: Ca2+ responses to thyrotropin-releasing hormone and angiotensin II: the role of plasma membrane integrity and effect of G11alpha protein overexpression on homologous and heterologous desensitization. *Cell Biochem Funct* **26**: 264-274, 2008.

OSTASOV P, SYKORA J, BREJCHOVA J, OLSZYNSKA A, HOF M, SVOBODA P: FLIM studies of 22- and 25-NBD-cholesterol in living HEK293 cells; plasma membrane change induced by cholesterol depletion. *Chem Phys Lipids* **167-168**: 62-69, 2013.

OSTROM RS, POST SR, INSEL PA: Stoichiometry and compartmentation in G protein-coupled receptor signaling: implications for therapeutic interventions involving G(s). *J Pharmacol Exp Ther* **294**: 407-412, 2000.

OSTROM RS, GREGORIAN C, DRENAN RM, XIANG Y, REGAN JW, INSEL PA: Receptor number and caveolar co-localization determine receptor coupling efficiency to adenylyl cyclase. *J Biol Chem* **276**: 42063-42069, 2001.

OSTROM RS, INSEL PA: The evolving role of lipid rafts and caveolae in G protein-coupled receptor signaling: implications for molecular pharmacology. *Br J Pharmacol* **143**: 235-245, 2004.

PIKE LJ: Lipid rafts: heterogeneity on the high seas. *Biochem J* **378**: 281-292, 2004.

PIPPIG S, ANDEXINGER S, LOHSE MJ: Sequestration and recycling of beta 2-adrenergic receptors permit receptor resensitisation. *Mol Pharmacol* **47**: 666-676, 1995.

PRESTON KL: Drug abstinence effects: opioids. *Br J Addict* **86**: 1641-1646, 1991.

PUCADYIL TJ, CHATTOPADHYAY A: Cholesterol modulates ligand binding and G-protein coupling to serotonin(1A) receptors from bovine hippocampus. *Biochim Biophys Acta* **1663**: 188-200, 2004.

PUCADYIL TJ, CHATTOPADHYAY A: Cholesterol depletion induces dynamic confinement of the G-protein coupled serotonin(1A) receptor in the plasma membrane of living cells. *Biochim Biophys Acta* **1768**: 655-668, 2007.

QUINTON TM, KIM S, JIN J, KUNAPULI SP: Lipid rafts are required in Galpha(i) signaling downstream of the P2Y12 receptor during ADP-mediated platelet activation. *J Thromb Haemost* **3**: 1036-1041, 2005.

RICHELSON E: Lithium ion entry through the sodium channel of cultured mouse neuroblastoma cells: a biochemical study. *Science* **196**: 1001-1002, 1977.

ROBINSON TE, KOLB B: Morphine alters the structure of neurons in the nucleus accumbens and neocortex of rats. *Synapse* **33**: 160-162, 1999.

RYBIN VO, XU X, LISANTI MP, STEINBERG SF: Differential targeting of beta-adrenergic receptor subtypes and adenylyl cyclase to cardiomyocyte caveolae. A mechanism to functionally regulate the cAMP signaling pathway. *J Biol Chem* **275**: 41447-41457, 2000.

RYBIN VO, PAK E, ALCOTT S, STEINBERG SF: Developmental changes in beta2-adrenergic receptor signaling in ventricular myocytes: the role of Gi proteins and caveolae microdomains. *Mol Pharmacol* **63**: 1338-1348, 2003.

SABOURIN T, BASTIEN L, BACHVAROV DR, MARCEAU F: Agonist-induced translocation of the kinin B(1) receptor to caveolae-related rafts. *Mol Pharmacol* **61**: 546-553, 2002.

SAVI P, ZACHAYUS JL, DELESQUE-TOUCHARD N, LABOURET C, HERVÉ C, UZABIAGA MF, PEREILLO JM, CULOUSCOU JM, BONO F, FERRARA P, HERBERT JM: The active metabolite of Clopidogrel disrupts P2Y12 receptor oligomers and partitions them out of lipid rafts. *Proc Natl Acad Sci USA* **103**: 11069-11074, 2006.

SCHEIDT HA, MULLER P, HERRMANN A, HUSTER D: The potential of fluorescent and spin-labeled steroid analogs to mimic natural cholesterol. *J Biol Chem* **278**: 45563-45569, 2003.

SCHWENCKE C, OKUMURA S, YAMAMOTO M, GENG YJ, ISHIKAWA Y: Colocalization of beta-adrenergic receptors and caveolin within the plasma membrane. *J Cell Biochem* **75**: 64-72, 1999.

SIBLEY DR, BENOVIC JL, CARON MG, LEFKOWITZ RJ: Molecular mechanisms of beta-adrenergic receptor desensitization. *Adv Exp Med Biol* **221**: 253-273, 1987.

SIMONS K, IKONEN E: Functional rafts in cell membranes. *Nature* **387**: 569-572, 1997.

STADEL JM, STRULOVICI B, NAMBI P, LAVIN TN, BRIGGS MM, CARON MG, LEFKOWITZ RJ: Desensitization of the beta-adrenergic receptor of frog erythrocytes. Recovery and characterization of the down-regulated receptors in sequestered vesicles. *J Biol Chem* **258**: 3032-3038, 1983.

SVOBODA P, TEISINGER J, NOVOTNY J, BOUROVA L, DRMOTA T, HEJNOVA L, MORAVCOVA Z, LISY V, RUDAJEV V, STOHR J, VOKURKOVA A, SVANDOVA I, DUSRCHANKOVA D: Biochemistry of trans-membrane signaling mediated by trimeric G-proteins. *Physiol Res* **53** (Suppl 1): S141-S152, 2004.

SYKORA J, BOUROVA L, HOF M, SVOBODA P: The effect of detergents on trimeric G-protein activity in isolated plasma membranes from rat brain cortex; correlation with studies of DPH and Laurdan fluorescence. *Biochim Biophys Acta* **1788**: 324-332, 2009.

UJCIKOVA H, DLOUHA K, ROUBALOVA L, VOSAHLIKOVA M, KAGAN D, SVOBODA P: Up-regulation of adenylylcyclases I and II induced by long-term adaptation of rats to morphine fades away 20 days after morphine withdrawal. *Biochim Biophys Acta* **1810**: 1220-1229, 2011.

USHIO-FUKAI M, HILENSKI L, SANTANAM N, BECKER PL, MA Y, GRIENDLING KK, ALEXANDER RW: Cholesterol depletion inhibits epidermal growth factor receptor transactivation by angiotensin II in vascular smooth muscle cells: role of cholesterol-rich microdomains and focal adhesions in angiotensin II signaling. *J Biol Chem* **276**: 48269-48275, 2001.

VON ZASTROW M, KOBILKA BK: Ligand-regulated internalization and recycling of human beta2-adrenergic receptors between the plasma membrane and endosomes containing transferrin receptors. *J Biol Chem* **267**: 3530-3538, 1992.

VON ZASTROW M, KOBILKA BK: Antagonist-dependent and -independent steps in the mechanism of adrenergic receptor internalization. *J Biol Chem* **269**: 18448-18452, 1994.

VOSAHLIKOVA M, SVOBODA P: The influence of monovalent cations on trimeric G protein G(i)1α activity in HEK293 cells stably expressing DOR-G(i)1α (Cys(351)-Ile(351)) fusion protein. *Physiol Res* **60**: 541-547, 2011.

WALDO GL, NORTHUP JK, PERKINS JP, HARDEN TK: Characterization of an altered membrane form of the beta-adrenergic receptor produced during agonist-induced desensitization. *J Biol Chem* **258**: 13900-13908, 1983.

WHISTLER JL, VON ZASTROW M: Morphine-activated opioid receptors elude desensitization by beta-arrestin. *Proc Nat Acad Sci USA* **95**: 9914-9919, 1998.

WHISTLER JL, CHUANG HH, CHU P, JAN LY, VON ZASTROW M: Functional dissociation of μ-opioid receptor signaling and receptor endocytosis: implications for the biology of opiate tolerance and addiction. *Neuron* **23**: 737-746, 1999.

XU W, YOON SI, HUANG P, WANG Y, CHEN C, CHONG PL, LIU-CHEN LY: Localization of the kappa opioid receptor in lipid rafts. *J Pharmacol Exp Ther* **317**: 1295-1306, 2006.

YOUNG W: Review of lithium effects on brain and blood. *Cell Transplant* **18**: 951-975, 2009.